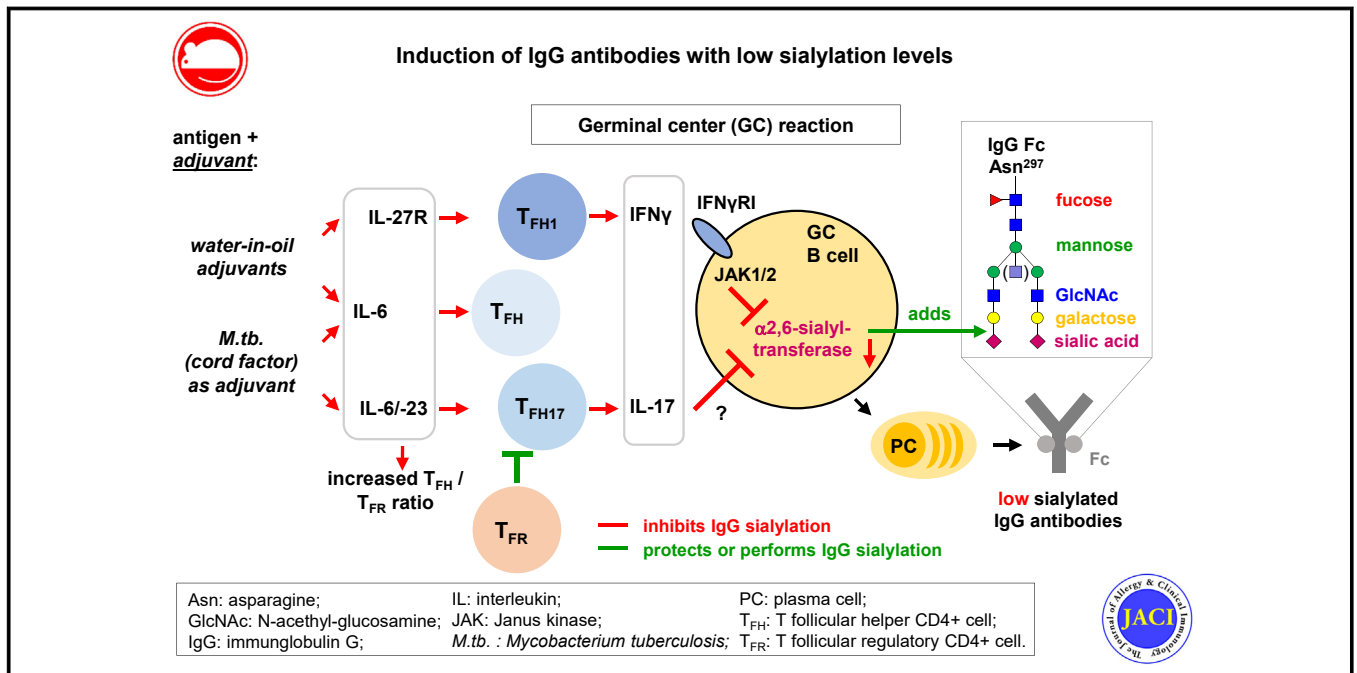# IgG Fc sialylation is regulated during the germinal center reaction following immunization with different adjuvants

Check for updates

Yannic C. Bartsch, PhD,[a]* Simon Eschweiler, PhD,[a]* Alexei Leliavski, PhD,[a]* Hanna B. Lunding, MSc,[a]*
Sander Wagt, MSc,[a,b]* Janina Petry, PhD,[a] Gina-Maria Lilienthal, PhD,[a] Johann Rahmöller, MD,[a,c] Noortje de Haan, PhD,[b]
Alexandra Hölscher, Tech,[d] Raghu Erapaneedi, PhD,[e] Anastasios D. Giannou, MD,[f] Lilian Aly, MD,[g] Ryota Sato, MSc,[h]
Louise A. de Neef,[b] André Winkler, PhD,[a,i] Dominique Braumann, MSc,[a,j] Juliane Hobusch, PhD,[a] Kyra Kuhnigk, MSc,[a]
Vanessa Krémer, MSc,[a] Moritz Steinhaus,[a] Véronique Blanchard, PhD,[j] Timo Gemoll, PhD,[k] Jens K. Habermann, PhD,[k]
Mattias Collin, PhD,[l] Gabriela Salinas, PhD,[m] Rudolf A. Manz, PhD,[n] Hidehiro Fukuyama, PhD,[h] Thomas Korn, PhD,[g,o]
Ari Waisman, PhD,[p] Nir Yogev, PhD,[q] Samuel Huber, MD,[f] Björn Rabe, PhD,[r] Stefan Rose-John, PhD,[r] Hauke Busch, PhD,[s]
Friederike Berberich-Siebelt, PhD,[e,t] Christoph Hölscher, PhD,[d,u] Manfred Wuhrer, PhD,[b] and Marc Ehlers, PhD[a,i,v]

Lübeck, Borstel, Würzburg, Hamburg, Berlin, Göttingen, Mainz, Cologne, and Kiel, Germany; Leiden, The Netherlands; Yokohama, Kanagawa, Japan; and Lund, Sweden

GRAPHICAL ABSTRACT

Background: Effector functions of IgG Abs are regulated by their Fc *N*-glycosylation pattern. IgG Fc glycans that lack galactose and terminal sialic acid residues correlate with the severity of inflammatory (auto)immune disorders and have also been linked to protection against viral infection and discussed in the context of vaccine-induced protection. In contrast, sialylated IgG Abs have shown immunosuppressive effects.

Objective: We sought to investigate IgG glycosylation programming during the germinal center (GC) reaction following immunization of mice with a foreign protein antigen and different adjuvants.

Methods: Mice were analyzed for GC T-cell, B-cell, and plasma cell responses, as well as for antigen-specific serum IgG subclass titers and Fc glycosylation patterns.

Results: Different adjuvants induce distinct IgG$^+$ GC B-cell responses with specific transcriptomes and expression levels of the α2,6-sialyltransferase responsible for IgG sialylation that correspond to distinct serum IgG Fc glycosylation patterns. Low IgG Fc sialylation programming in GC B cells was overall highly dependent on the Foxp3$^-$ follicular helper T (T_{FH}) cell–inducing cytokine IL-6, here in particular induced by water-in-oil adjuvants and *Mycobacterium tuberculosis*. Furthermore, low IgG Fc sialylation programming was dependent on adjuvants that induced IL-27 receptor–dependent IFN-γ$^+$ T_{FH1} cells, IL-6/IL-23–dependent IL-17A$^+$ T_{FH17} cells, and high ratios of T_{FH} cells to Foxp3$^+$ follicular regulatory T cells. Here, the 2 latter were dependent on *M tuberculosis* and its cord factor.

Conclusion: This study's findings regarding adjuvant-dependent GC responses and IgG glycosylation programming may aid in the development of novel vaccination strategies to induce IgG Abs with both high affinity and defined Fc glycosylation patterns in the GC. (J Allergy Clin Immunol 2020;146:652-66.)

Key words: Antibodies, IgG glycosylation, vaccination, adjuvants, germinal center, T follicular cells, IL-6, IL-27R, IL-17, IFN-γ

Abbreviations used

BM:	Bone marrow
CFA:	Complete Freund adjuvant
DC:	Dendritic cell
eCFA:	Enriched complete Freund adjuvant
G0:	Agalactosylated
GC:	Germinal center
HRP:	Horseradish peroxidase
IFA:	Incomplete Freund adjuvant
IL-27R:	IL-27 receptor
KO:	Knockout
MPLA:	Monophosphoryl lipid A
Mtb:	*Mycobacterium tuberculosis*
Ova:	Ovalbumin
PC:	Plasma cell
Poly(I:C):	Polyinosinic-polycytidylic acid
RA:	Rheumatoid arthritis
St6gal1:	α2,6-Sialyltransferase 1
TDB:	Trehalose-6,6-dibehenate
T_{FH} cell:	Foxp3$^-$ follicular helper T cell
T_{FR} cell:	Foxp3$^+$ follicular regulatory T cell
TLR:	Toll-like receptor
WT:	Wild-type

IgG Abs play a central role in the immune defense against pathogens. Vaccination efficiency is usually assessed by the amount of induced IgG Abs, their Fab-dependent affinity, and (if necessary) their neutralizing capacity.[1] Germinal center (GC)-derived IgG Abs attract particular attention because IgG hypermutations occur especially in GC B cells and GC responses generate memory B cells as well as long-lived plasma cells (PCs).[2-5] On the other hand, the Fc-mediated effector functions of IgG Abs depend on the IgG subclass and type of Fc *N*-glycosylation.[1,6-20] The biantennary *N*-glycan is coupled to Asn 297 in the CH2 domain of both IgG heavy chains and consists of a 7-monosaccharide core structure that can be modified by the attachment of fucose, bisecting acethylglucosamine (GlcNAc), β1,4–linked galactose, and α2,6–linked terminal sialic acid (Fig 1).[7]

There is a general consensus that agalactosylated (G0), afucosylated, and bisected IgG Abs are linked to inflammatory conditions, whereas galactosylated and sialylated IgG Abs are correlated with ameliorated inflammatory conditions.[6-13,15,16,19-21] Furthermore, anti-inflammatory effector functions have been described for sialylated bulk and antigen-specific IgG Abs.[7-9,11,15,18,20,21]

Functionally, the type of IgG Fc glycosylation influences the interaction and affinity of IgG Abs with the complement molecules, classical Fcγ receptors (type I Fc receptors), and nonclassical type II Fc receptors (a group that includes sugar-binding C-type lectin receptors).[7,8,10,13,14,18,21]

Dynamic changes in IgG Fc glycosylation have been linked to progression or amelioration (ie, after therapy or during pregnancy) of several autoimmune and inflammatory disorders, such

https://doi.org/10.1016/j.jaci.2020.04.059

FIG 1. Adjuvants induce distinct IgG subclass titer and Fc glycosylation patterns after immunization with a foreign protein antigen. **A,** The experimental design was as follows: C57BL/6 WT female mice were immunized with Ova plus distinct adjuvants and boosted with Ova without adjuvant on day 28 (n = 5 per group). **B,** The investigated adjuvants with their color codes. **C,** Serum titers of anti-Ova total IgG and IgG subclasses on the indicated time points (the serum dilutions used are shown). **D,** Schematic structures of 2 possible IgG Fc N-glycans coupled to asparagine (Asn) 297. The biantennary G0 core structure (4 GlcNAcs and 3 mannoses; G0; mostly with fucose and without bisecting GlcNAc) can be further modified with galactose (Gal; G) and sialic acid (Sial; S) (eg, G2S2). **E,** Serum anti-Ova IgG1 and IgG2 (IgG2c + IgG2b) Fc agalactosylation (percentages of the corresponding glycopeptide [G0]) and sialylation (G1S1 + G2S1 + G3S1 + G2S2) at the indicated time points. Several IgG2 signals were too low for a reliable analysis and therefore excluded. Horizontal dashed lines indicate average bulk serum IgG1 or IgG2 glycosylation before immunization; vertical lines represent the Ova boost on day 28.

as rheumatoid arthritis (RA).[15,16] This indicates that the type of IgG Fc glycosylation is actively regulated and reflects the inflammatory state of the host's immune response.

IgG Fc galactosylation and sialylation are regulated by 2 glycosyltransferases, β1,4-galactosyltransferase 1 (B4galt1) and α2,6-sialyltransferase 1 (St6gal1), respectively.[9,11,12,15,16,20,21] Genetic deletion of *St6gal1* in activated class-switched B cells (*AID-Cre × St6gal1^fl/f* mice) has highly reduced Fc sialylation of autoantigen-specific IgG Abs and exacerbated inflammatory responses, indicating that IgG Fc sialylation is primarily regulated in IgG-producing B cells.[15]

By using models of chronic autoimmunity, another study has revealed that the inflammatory cytokine IL-23 plays an important role in establishing low St6gal1 expression levels in Ab-producing cells and low sialylated IgG autoantibodies.[16] These authors have proposed that IL-23–dependent pathogenic T_H17 cells, which play a crucial role in chronic autoimmune inflammation,[22] may induce IgG autoantibodies with low sialylation levels.[16]

On the contrary, much less is known about the role of glycosylation in IgG Fc-mediated protection against infections.[1,17] Notably, recent studies have linked G0 IgG Abs to protective immune responses during HIV infection and subsequent to vaccination.[23,24] Hence, it has been suggested that distinct vaccination strategies and adjuvants may have a substantial influence not only on the IgG titer and subclass but also on the type of Fc N-glycosylation.[1,9,11,17,18,24-26] However, the cellular and molecular pathways responsible for IgG glycosylation programming following immunization (eg, after immunization with different adjuvants) are still barely investigated.[1,17]

Here, we immunized mice with a foreign protein and different adjuvants to investigate the development of the adjuvant-induced IgG Fc glycosylation patterns. We identified several lines of evidence that different adjuvants program GC B-cell responses with distinct transcriptomes, and in particular, St6gal1 expression levels. In this context, we revealed that low IgG Fc sialylation programming in GC B cells was, overall, dependent on the

Foxp3$^-$ follicular helper T (T$_{FH}$) cell–inducing cytokine IL-6. Further, low IgG Fc sialylation programming was dependent on IL-27 receptor (IL-27R)-dependent IFN-γ$^+$ T$_{FH1}$ cells, IL-6/IL-23–dependent IL-17A$^+$ T$_{FH17}$ cells and high T$_{FH}$ cell–to–Foxp3$^+$ follicular regulatory T (T$_{FR}$) cell ratios.

METHODS
Mice

C57BL/6 wild-type (WT) mice were purchased from Charles River Laboratories or The Jackson Laboratory and bred in our mouse house facilities. IL-6–deficient (IL-6 knockout [KO], IL-6 flox/flox [fl/fl], and IL-6 fl/fl × CD11c-Cre/WT [Tg(Itgax-cre)]$^{1–1Reiz}$) mice (from Jackson Laboratory); IL-23p19 KO mice, IL-27R KO (WSX-1 KO) mice, IL-17A-EGFP reporter mice; IL-17A KO mice; and IFN-γRI KO mice have been developed as described and backcrossed for a minimum of 8 generations to the C57BL/6 background.[27-34] Sex-matched 8- to 12-week-old mice were used in the same experiments. The experiments were conducted according to the German animal protection laws and approved by the animal research ethics boards of the corresponding ministries in Germany.

Reagents

Ovalbumin (Ova) (grade VI; catalog no. A2512), incomplete Freund adjuvant (IFA) (catalog no. F5506), complete Freund adjuvant (CFA) (catalog no. F5881; 1 mg of *Mycobacterium tuberculosis* [Mtb]/mL), and LPS (from *Escherichia coli* 0111:B4; catalog no. L3012) were obtained from Sigma-Aldrich (St. Louis, Mo). Enriched CFA (eCFA) was prepared by adding heat-killed Mtb.H37 RA (BD Biosciences, San Diego, Calif) to IFA (5 mg of Mtb/mL). Alum (alhydrogel adjuvant 2%; catalog identifier vac-alu), Adju-Phos (Adju-Phos adjuvant; catalog identifier vac-phos), AddaVax (catalog identifier vac-adx), R848 (R848 VacciGrade; catalog no. vac-r848), monophosphoryl lipid A (MPLA) (MPLA-SM VacciGrade; catalog identifier vac-mpla), polyinosinic-polycytidylic acid (Poly(I:C)) (HMW) VacciGrade; catalog identifier vac-pic) and trehalose-6,6-dibehenate (TDB) (TDB VacciGrade; catalog identifier vac-tdb [TDB is a nontoxic synthetic analog of the mycobacterial cell wall component trehalose 6,6'-dimycolate]), and TDB-HS15 (TDB formulated with Kolliphor HS 15, which is a potent low-toxicity nonionic solubilizer; catalog identifier tlrl-stdb) were purchased from InvivoGen (Toulouse, France). Montanide (catalog no. Montanide ISA 51 VG) was purchased from Seppic (Paris, France). Alum plus Mtb was prepared by adding heat-killed Mtb.H37 RA to alum (5 mg of Mtb/mL).

Ova immunizations

Mice were immunized intraperitoneally with 100 μg of Ova plus the indicated adjuvant in a total volume of 200 μL; therefore, 100 μL of the adjuvant solution (eg, R848 [100 μg], Poly(I:C) [100 μg], LPS [30 μg], MPLA [10 μg], TDB [100 μg], or TDB-HS15 [100 μg]) and 100 μL of an Ova-PBS solution (200 μg/mL) were mixed before immunization. In boost experiments, mice were boosted intraperitoneally with 100 μg of Ova in 200 μL of PBS without adjuvant.

Ova-reactive ELISA

ELISA plates were coated with 10 μg/mL or 1 μg/mL of Ova to measure the reactivity of the indicated serum anti-Ova IgG subclass Abs. After incubation with the indicated serum dilutions, bound Abs were detected with horseradish peroxidase (HRP)-coupled polyclonal goat anti-mouse IgM-specific, IgG-Fc-specific, IgG1-specific, IgG2c-specific (the isoform of IgG2a in C57BL/6 mice), IgG2b-specific, or IgG3-specific Abs purchased from Bethyl Laboratories (Montgomery, Tex). After incubation with the 3,3′,5,5′-tetramethylbenzidine (TMB) substrate (BD Biosciences, San Diego, Calif), the OD was measured at 450 nm.

Purification of bulk and serum anti-Ova IgG Abs

For bulk IgG preparation, serum samples were purified with protein G coupled to Sepharose (GE Healthcare). Serum anti-Ova IgG Abs were purified by using Ova coupled to cyanogen bromide–activated Sepharose 4B (GE Healthcare) prepared in our laboratory.

IgG Fc subclass glycopeptide analysis via nano–liquid chromatography–mass spectrometry

Murine IgG Fc subclass glycopeptides were analyzed by nano–liquid chromatography–mass spectrometry, as described previously.[18,35] In short, purified bulk or anti-Ova IgG Abs were cleaved with trypsin and analyzed by nano–liquid chromatography–mass spectrometry. On the basis of the terminal sugar moiety, the IgG1, IgG2 (IgG2c and IgG2b glycopeptides cannot be distinguished), and IgG3 subclass–specific Fc *N*-glycopeptide peak areas were background-corrected, summed (100%), and assigned (percent of 100) to 1 of the following 9 groups: G0, G1, G2, G3, G4, G1S1, G2S1, G3S1, and G2S2.

Flow cytometric analysis

Spleen or bone marrow (BM) cells from immunized and untreated mice or cultured cells were prepared for flow cytometric analysis (LSRII, BD Biosciences and Attune Nxt, Thermo Fisher Scientific) on the indicated days. The following biotin- or fluorochrome-coupled Abs or Ova were used for surface staining at 4 °C: anti-B220 (BD Bioscience, clone RA3-6B2), anti-CD95 (FAS; BD Biosciences, Jo-2), anti-CD138 (BD Biosciences, 281-2), anti-IgG1 (BioLegend, RMG1-1), anti-IgM (eBiosciences, eB121-15F9), anti-IgG-Fc (Bethyl, polyclonal), anti-CD4 (Biolegend, RM4-5), anti-CD8 (BioLegend, 53-6.7), anti–CXCR-5 (BioLegend, L138D7), anti–GL-7 (BioLegend, GL-7), anti-ICOS (BioLegend, C398.4A), streptavidin (BioLegend), and Ova (fluorochrome-coupled, Thermo Fisher Scientific). For intracellular staining, the samples were fixed with Cytofix/Cytoperm according to the manufacturer's instructions (BD Biosciences) followed by permeabilization with permeabilization/wash buffer (our own preparation [0.05% saponin in 0.05 × PBS]). Samples were then intracellularly stained with anti-IgG1 (BioLegend, RMG1-1), anti-IgM (eBiosciences, eB121-15F9), anti-IgG-Fc (Bethyl, polyclonal), anti-St6gal1 (R&D Systems, polyclonal goat IgG Ab), or isotype goat control IgG (R&D Systems), streptavidin (BioLegend), and Ova (fluorochrome-coupled, Thermo Fisher Scientific). For intracellular cytokine analysis (anti–IFN-γ (BD Biosciences, XMG1.2), anti–IL-17A (BD Biosciences, TC11-18H10 or eBioscience, eBio17B7), cells were restimulated before analysis with a cell stimulation cocktail containing phorbol myristate acetate and ionomycin plus protein transport inhibitors according to the manufacturer's instructions (eBioscience, 00-4975-93). Samples were intranuclearly stained with anti-Foxp3 (FJK16s, eBioscience) according to the manufacturer's instructions (eBioscience).

B-cell culture

Murine splenic B cells were isolated by negative selection using the mouse B-cell isolation kit (Miltenyi Biotec) with B-cell purity (B220$^+$ cells) greater than 95%. Purified B cells (6-8 × 10^4/mL) were cultured in ʟ-glutamine–containing RPMI-1640 medium (Thermo Fisher Scientific) supplemented with 10% FCS (Gibco, Thermo Fisher Scientific), 50 μM 2-mercaptoethanol (Sigma-Aldrich), 1 mM HEPES (Sigma-Aldrich), and 100 U/mL of penicillin/streptomycin (Gibco, Thermo Fisher Scientific) at 37°C and 5% CO$_2$. B cells were treated with 2.5 μg/mL of LPS (from *E. coli* 0111:B4; Sigma-Aldrich) and recombinant murine IFN-γ (catalog no. 315-05; Peprotech). On day 4, St6gal1 protein expression was measured in IgG$^+$ B cells by flow cytometry and in total B cells by Western blot (equal amounts of cultured cells [1-2 × 10^6] from every treatment were used for analyses). The JAK1/JAK2 inhibitor Ruxolitinib (catalog no. S1378) was purchased from Selleckchem.

Western blot

Cultured cells (2×10^6) were pelleted and lysed in radioimmunoprecipitation assay buffer (150 mM NaCl, 1 % NP-40, 0.1 % SDS, 50 mM Tris, and 0.5 % sodium deoxycholate) supplemented with a protease inhibitor cocktail (Roche). The protein concentration was determined by using a Pierce BCA Protein Assay Kit (Thermo Fisher Scientific). Equal amounts of protein (2 μg) were taken up in a reducing buffer and separated by SDS-PAGE. The protein was then transferred to a polivinylidene difluoride membrane by using the Trans-Blot Turbo Transfer System (Bio-Rad). The membranes were blocked with 5% nonfat milk in TBS-Tween20 and incubated with primary Abs against St6gal1 (AF5924, R&D Systems) and glyceraldehyde-3-phosphate dehydrogenase (AF5718, R&D Systems). For detection, membranes were incubated with anti-goat HRP-conjugated Abs and developed with Immoblion Western HRP Substrate (WBKLS0050, Millipore).

mRNA sequencing and bioinformatic analyses

C57BL/6 WT mice were immunized with 100 μg of Ova in eCFA (Ova-eCFA) or LPS (Ova-LPS), as already described. On day 8, splenic IgG1$^+$IgM$^-$ GC B cells (B220$^+$CD138$^-$GL7$^+$FAS$^+$) were sorted on a FACSAria II (BD Biosciences), and total RNA was isolated by using a TRIzol (Invitrogen)-based protocol according to the manufacturer's recommendations (Invitrogen). Library preparation for mRNA sequencing was performed by using the TruSeq mRNA Sample Preparation Kit from Illumina (catalog no. RS-122-2101), starting from 100 ng of total RNA. Accurate quantification of cDNA libraries was performed by using the QuantiFluor dsDNA System (Promega). cDNA libraries were amplified and sequenced by using the cBot and HiSeq4000 from Illumina (SR, 1 × 51 bp, 4 GB per sample). Using the Illumina software BaseCaller, sequence images were transformed to bcl files, which were demultiplexed to fastq files by using bcl2fastq (version 2.17). The generated raw reads were then mapped to the reference mouse genome (version GRCm38.p4) sourced from the Ensembl database by using STAR software (version 2.5).[36] Read counts for each transcript were obtained by using feature-Counts,[37] which quantifies the reads generated from sequenced RNA. To estimate normalized gene expression, the conditional quantile normalization method was used.[38] Differentially expressed genes were identified by using the Bioconductor software package DESeq2[38] with a Benjamini-Hochberg adjusted P value cutoff of .05. Gene set enrichment analysis was performed with the R/Bioconductor software package GAGE[39] using mouse ortholog-converted gene sets from the Molecular Signatures Database (http://bioinf.wehi.edu.au/software/MSigDB). Heatmaps were generated by using the heatmap function in the NMF package, whereas the package ggplot2 was used for making principal component analysis, minus-average, and volcano plots. Gene set enrichment analyses were done with the hallmark gene sets[40] and the Reactome (https://reactome.org/) and KEGG (https://www.genome.jp/kegg/) pathway databases.

Data availability

The mRNA data are available at the National Center for Biotechnology Information Sequence Read Archive database under the BioProject and BioSample number: PRJNA352913.

Statistical analysis

Statistical analyses were performed by using GraphPad Prism software, version 6.0 (GraphPad, La Jolla, CA). For the small sample sizes, normal distribution was assumed. To analyze differences between 2 normally distributed groups or between more than 2 groups, respectively, the 2-tailed Student t test or 1-way ANOVA was used. A P value less than .05 was considered to indicate a significant difference (*P < .05; **P < .01; and ***P < .001). If not stated otherwise, murine data were taken from 1 representative experiment of 2 to 5 individual experiments or combined from multiple experiments and presented as the mean or median (median fluorescence intensity) values, as indicated, plus or minus SEM. Graph points indicate individual mice.

RESULTS

Adjuvants differ in their ability to program antigen-specific IgG glycosylation patterns

To establish an *in vivo* immunization system for studying IgG Fc *N*-glycosylation programming, we investigated the potential of a broad panel of adjuvants and costimuli in combination with the classical T-cell–dependent foreign protein antigen Ova for their ability to induce Ova-specific IgG subclass titers and Fc *N*-glycosylation patterns in C57BL/6 WT female mice (Fig 1 and see Figs E1 and E2 in this article's Online Repository at www.jacionline.org).

As immunogenic costimuli, we applied adjuvants used in preclinical research (the water-in-oil adjuvant IFA, IFA enriched with Mtb (eCFA containing 5 mg/mL Mtb) and adjuvants presently used for human vaccination (the water-in-oil adjuvant Montanide, alum [aluminum hydroxide], Adju-Phos [aluminum phosphate], and AddaVax [a squalene-based oil-in-water nanoemulsion with a formulation similar to that of MF-59]) as well as several Toll-like receptor (TLR) agonists (the TLR4 agonists LPS and MPLA, the TLR7 and TLR8 agonist R848 [Resiquimod], and the TLR3 agonist Poly(I:C)) (Fig 1, B and see Figs E1 and E2).

All groups were additionally boosted with Ova without adjuvant on day 28. Sera were collected on the indicated days (Fig 1, A and see Figs E1 and E2).

The water-in oil adjuvants eCFA and IFA were most potent in inducing anti-Ova IgG Abs, followed by the water-in oil adjuvant Montanide and alum and Adju-Phos (Fig 1 and see Figs E1 and E2). Although anti-Ova IgG titers were initially low for AddaVax, LPS, MPLA, R848, and Poly(I:C), boosting with Ova on day 28 augmented the anti-Ova IgG production in these groups, indicating a reactivation of initially primed memory B-cell responses (Fig 1, C and see Figs E1 and E2).

Most adjuvants induced predominantly anti-Ova IgG Abs of the IgG1 subclass. In addition, eCFA and IFA also induced anti-Ova IgG2c (the IgG2a haplotype of C57BL/6 mice), IgG2b, and IgG3 Abs. Montanide also promoted IgG2b Abs, Poly(I:C) strongly induced IgG2c titers, and LPS and MPLA also induced IgG2c and IgG2b Abs, whereas aluminum-based adjuvants favored sole IgG1 production. Anti-Ova IgG3 Ab titers were in general low and, interestingly, seemed to not be boosted on day 28 (Fig 1, C and see Figs E1 and E2).

The Fc *N*-glycosylation patterns of serum anti-Ova IgG1 and IgG2 (both IgG2c and IgG2b, which could not be distinguished by the glycopeptide profiling method used) Abs were analyzed for all immunization groups on the indicated days and assigned to 1 of 9 glycopeptide groups (G0, G1, G2, G3, G4, G1S1, G2S1, G3S1, and G2S2) (Fig 1, D and E and see Fig E2). G3, G4, and G3S1 glycopeptide signals (carrying additional α1,3-linked terminal galactoses) and glycopeptides without fucose (F0) were detected for some samples, however, with peak area intensities always less than 3% or 2%, respectively. When observed, F0 glycopeptide signals were added to their corresponding 9 (fucosylated) glycopeptide counterparts. Glycopeptides containing bisecting GlcNAc were not detected. IgG3 and several IgG2 signals were too low for a reliable analysis and hence were excluded.

As recently reported,[18,26,35] galactosylation and sialylation levels of murine IgG2 Abs were in general higher than those of IgG1 Abs in the same sample of C57BL/6 mice (Fig 1, E and
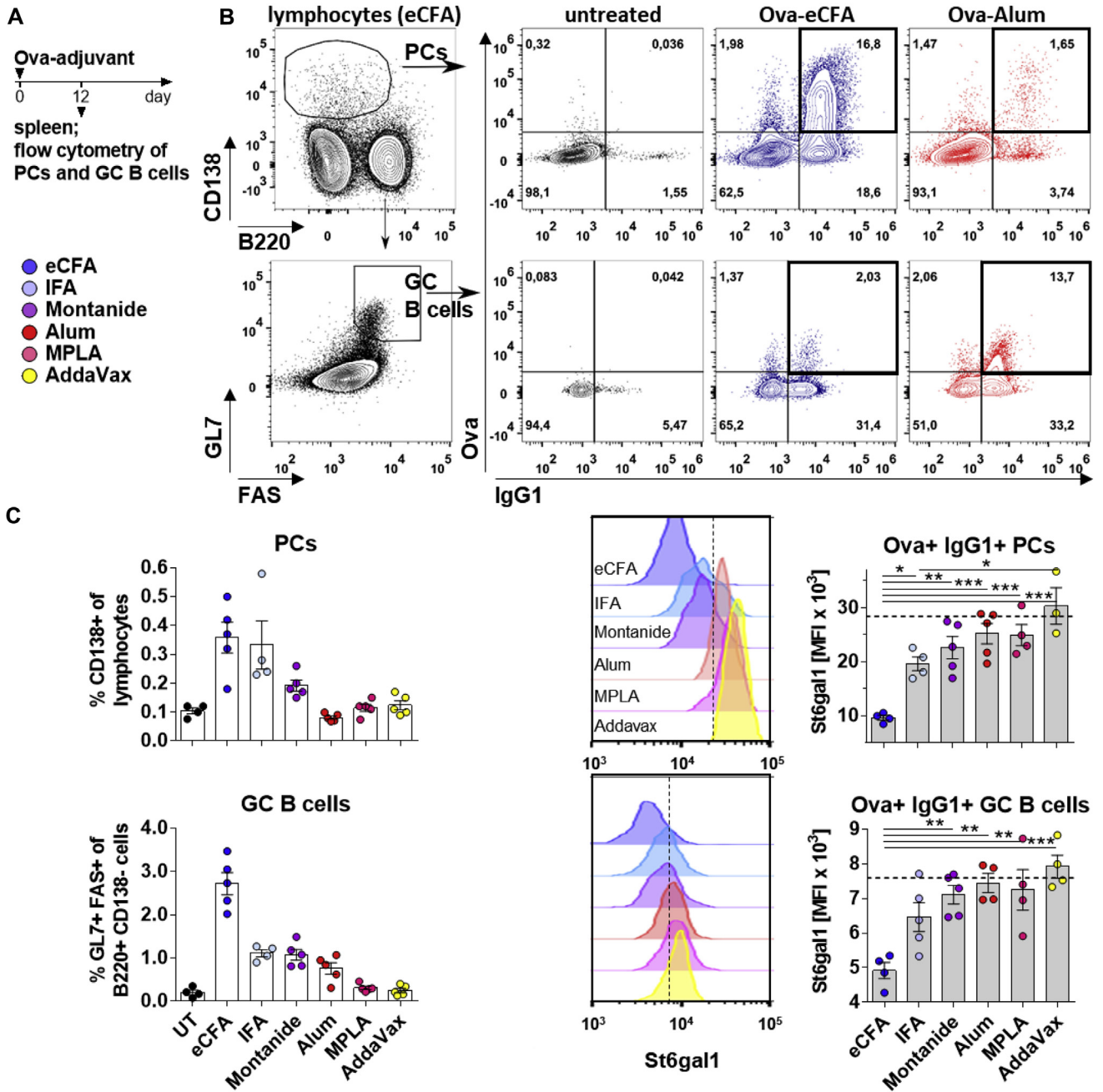
FIG 2. Adjuvants induce distinct St6gal1 protein expression levels in splenic antigen-specific IgG1^{+} PCs as well as in GC B cells. **A,** The experimental design was as follows: WT female mice were immunized with Ova plus distinct adjuvants (eCFA, IFA, Montanide, Alum, MPLA, or AddaVax, including their color codes) (n = 4 or 5 per group). For flow cytometry analysis, spleens were taken on day 12. **B,** Gating strategy to identify Ova-specific (Ova[+]) IgG1^{+} PCs and GC B cells (pregated on viable single lymphocytes) after Ova-eCFA and Ova-alum immunization compared with untreated (UT) controls. **C,** Frequencies of splenic PCs and GC B cells on day 12 (*left*) and intracellular St6gal1 protein expression (*right*) (median fluorescence intensity [MFI]), including overlay histograms of representative mice (*vertical lines are orientation guides*), in Ova-specific (Ova[+]) IgG1^{+} PC and GC B cells on day 12. Graph points indicate individual mice. Horizontal lines indicate average St6gal1 expression levels in IgG1^{+} PCs and GC B cells of UT mice. One of 2 independent experiments is shown.

see Fig E2), which was very likely due to higher accessibility of the IgG2b/c Fc glycosylation sites for the corresponding glycosyltransferases (our own observation after *in vitro* production of IgG subclass mAbs with the identical V(D)J sequence).

On day 7, early serum anti-Ova IgG Abs showed high levels of galactosylation and sialylation irrespective of the used adjuvant (Fig 1, *E* and see Fig E2). These early sialylated IgG Abs were likely produced by extrafollicular plasmablasts and might contribute to the transport of the antigen to the GC.[14,41]
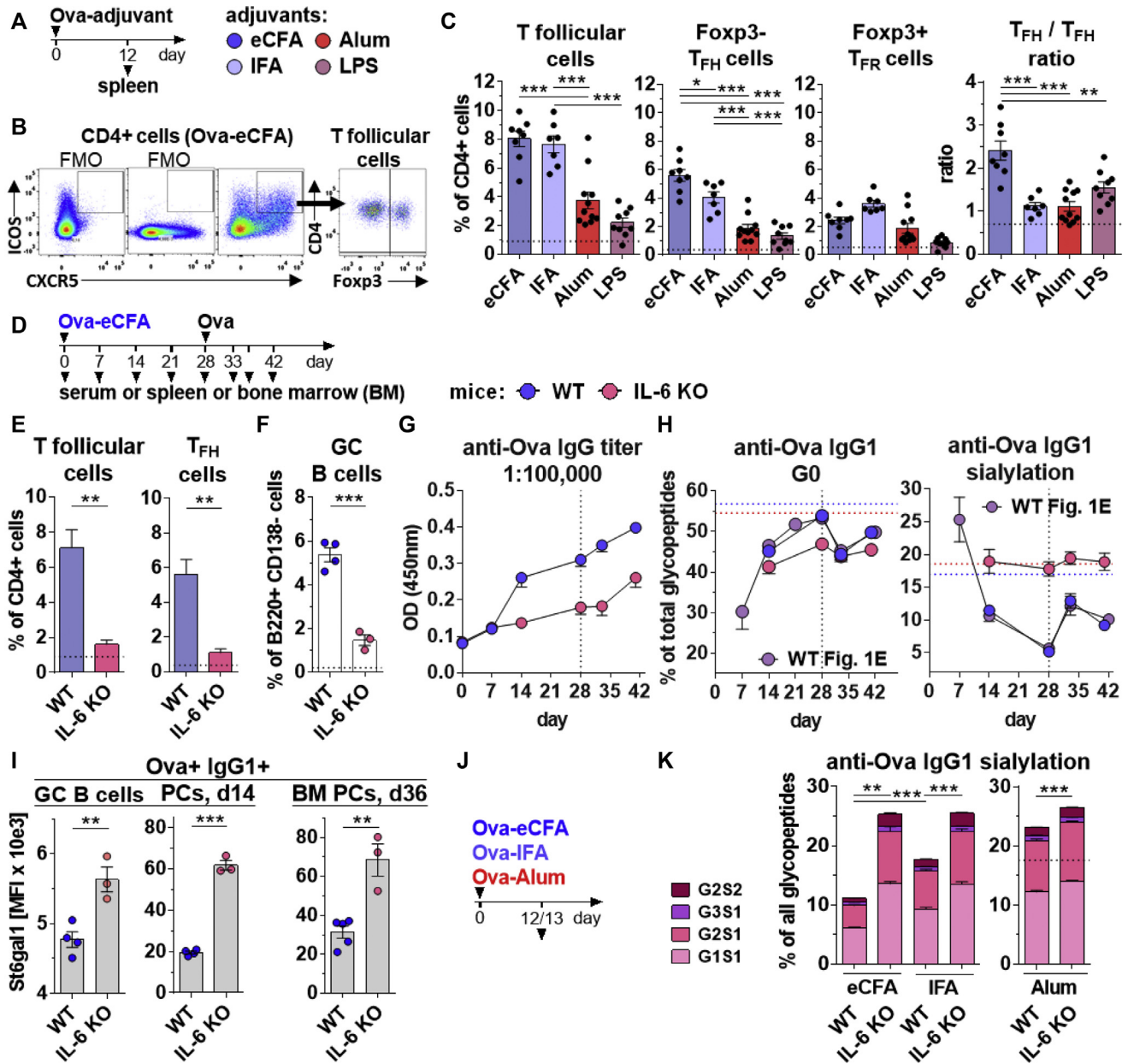
FIG 3. Adjuvants induce distinct IL-6–dependent T follicular cell responses and IgG Fc glycosylation patterns. **A,** The experimental design for (**B**) and (**C**) was as follows: WT female mice were immunized with Ova plus the indicated adjuvants and analyzed on day 12 (n = 4 or 5 per group). **B,** Gating strategy (including ICOS and CXCR5 FMOs [fluorescence minus 1 controls]) to identify splenic CXCR5$^+$ ICOS$^+$ T follicular, Foxp3$^-$ T$_{FH}$, and Foxp3$^+$ T$_{FR}$ cells. **C,** Frequencies of splenic T follicular, T$_{FH}$, and T$_{FR}$ cells and the T$_{FH}$ cell–to–T$_{FR}$ cell ratios. Horizontal dashed lines indicate average cell population frequencies of untreated mice. **D,** The experimental design for (**E**) to (**I**) was as follows: WT and IL-6 KO female mice were immunized with Ova-eCFA and boosted with Ova without adjuvant on day 28 (n = 3-5 per group). **E** and **F,** Frequencies of splenic T follicular, T$_{FH}$, and GL7$^+$ FAS$^+$ GC B cells on day 14. **G,** Serum titers of anti-Ova total IgG (serum dilution, 1:100,000). **H,** Serum anti-Ova IgG1 Fc agalactosylation (G0) and sialylation (G1S1 + G2S1 + G3S1 + G2S2) on the indicated time points. The WT data from Fig 1, *E* are shown for comparison. Horizontal dashed lines indicate average bulk IgG1 glycosylation before immunization. **I,** St6gal1 protein expression in splenic Ova-specific (Ova$^+$) IgG1$^+$ GC B cells and PCs on day 14 and BM PCs on day 36. **J,** The experimental design for (**K**) was as follows: WT and IL-6 KO female mice were immunized with Ova plus eCFA, IFA, or alum and analyzed on day 12 or 13 (n = 4 or 5 per group). **K,** Serum anti-Ova IgG1 sialylation. One of at least 2 independent experiments or (**C**) up to 3 summarized independent experiments are shown for each set of investigation.

From day 14 on, however, the potential of the distinct adjuvants became decisive in determining antigen-specific IgG subclass Fc glycosylation. Importantly, the anti-Ova IgG Fc glycosylation patterns could be used to divide the tested adjuvants into 3 groups. The water-in-oil adjuvants Montanide and, in particular, IFA (group 1) substantially reduced the galactosylation and sialylation levels of serum anti-Ova IgG1 and IgG2 Abs. These anti-Ova IgG1 and IgG2 galactosylation and sialylation levels were even further reduced by the addition of Mtb to IFA (group 2; eCFA). In contrast, the other adjuvants (group 3) induced a clearly lower downregulation of the anti-Ova IgG subclass galactosylation and sialylation levels (Fig 1, *E* and see Fig E2).

Our results imply that the potential of different adjuvants to affect IgG glycosylation becomes apparent only when the IgG Ab response is mainly driven by GC-derived PCs.[4,5,14] Accordingly, we observed that Ova-eCFA immunization enhanced the affinity of the anti-Ova IgG Abs between day 8 and 14 (see Fig E1, *D* and *E* in this article's Online Repository at www.jacionline.org).[5] Importantly, the different trends in the anti-Ova IgG Fc glycosylation patterns after immunization with the distinct adjuvants were comparable between the IgG1 and IgG2 subclasses. This was also true for all subsequent experiments, implying common regulatory mechanisms for the different IgG subclasses.

Similar dynamics of serum anti-Ova IgG Fc glycosylation were observed after antigen reexposure without adjuvant on day 28. On day 33, the IgG Fc galactosylation and sialylation levels transiently increased again in all groups, suggesting a fast extrafollicular response by newly activated and in particular reactivated memory B cells.[3] On days 42 and 57, however, anti-Ova IgG Ab galactosylation and sialylation levels decreased again and showed comparable differences between the groups as observed before the boost (Fig 1, *E* and see Fig E2).

Differences in IgG Fc sialylation are reflected in the St6gal1 expression levels in Ova-specific IgG$^+$ PCs as well as in Ova-specific IgG$^+$ GC B cells

The expression of the α2,6-sialyltransferase, St6gal1, in activated B cells is necessary for proper IgG Fc sialylation.[15] In accordance, we found that the differences between the anti-Ova IgG subclass Fc glycosylation patterns of the eCFA, IFA, Montanide, alum, MPLA, and AddaVax groups from day 14 to 28 were comparable to those of the respective St6gal1 protein expression levels of Ova-specific IgG1$^+$ and IgG2/3$^+$ CD138$^+$ PCs as well as Ova-specific IgG1$^+$ and IgG2/3$^+$ GL7$^+$ FAS$^+$ GC B cells on day 12 (Fig 2 and see Figs E3 and E4 in this article's Online Repository at www.jacionline.org). Montanide and especially IFA tended to reduce, whereas addition of Mtb to IFA (eCFA) further significantly reduced the St6gal1 protein expression in antigen-specific IgG$^+$ GC B cells and PCs compared with that in the remaining immunization groups (Fig 2, *C* and see Figs E3 and E4). Furthermore, the significant differences in St6gal1 protein expression levels between the Ova-eCFA and Ova-alum groups were also observed in splenic and BM Ova-specific IgG1$^+$ CD138$^+$ PCs, following the boost, on day 36 (see Fig E5 in this article's Online Repository at www.jacionline.org).

Intriguingly, significant differences in St6gal1 protein expression in IgG1$^+$ GC B cells between the Ova-eCFA and Ova-alum groups were detectable not on day 8 but later on day 12 and 14 (Fig 2, see Fig E6 [available in this article's Online Repository at www.jacionline.org], and data not shown). St6gal1 expression

thereby decreased after Ova-eCFA immunization between day 8 and day 12 or 14. Together, these observations implied that St6gal1 protein expression in GC B cells is programmed during the GC reaction.

We then focused on immunizations with Ova-IFA and Ova-eCFA to learn about water-in-oil– and Mtb-induced signals leading to low St6gal1 expression and low anti-Ova IgG galactosylation and sialylation levels versus with Ova-alum or Ova-LPS immunizations, which induced higher St6gal1 expression and higher anti-Ova IgG galactosylation and sialylation levels.

Different adjuvants induce distinct T follicular cell responses

The GC B-cell response is regulated by CXCR5$^+$ ICOS$^+$ CD4$^+$ T follicular cells, which can be further subdivided into T$_{FH}$ cells and their regulatory counterparts, T$_{FR}$ cells.[4,5,42-44]

Here, the frequencies of T$_{FH}$ cells correlated roughly with the frequencies of GC B cells and inversely with the St6gal1 protein expression levels in antigen-specific IgG$^+$ GC B cells and PCs, as well as with the anti-Ova IgG subclass glycosylation levels after immunization with Ova-eCFA, Ova-IFA, Ova-alum, or Ova-LPS on day 12 (Figs 2 and 3, *A-C* and data not shown). These findings are in accordance with those of recent studies showing that water-in-oil adjuvants induce strong T$_{FH}$ responses.[45] Notably, the addition of Mtb to IFA (eCFA) further significantly enhanced the T$_{FH}$ response and increased the T$_{FH}$ cell–to–T$_{FR}$ cell ratio by a factor of 2 as compared with IFA without Mtb. These data implied that low St6gal1 expression in GC B cells after immunization with water-in-oil adjuvants as well as additional Mtb is regulated by the T follicular cell response.

The T$_{FH}$-inducing cytokine IL-6 is required for accumulation of IgG$^+$ GC B cells and PCs with low St6gal1 expression

To analyze the role of T$_{FH}$ cells in downregulating IgG Fc sialylation and St6gal1 expression, we next investigated the role of the cytokine IL-6, which is a major inducer of T$_{FH}$ cells.[45-49] Compared with WT controls, IL-6–deficient (IL-6 KO) mice showed highly reduced frequencies of splenic T follicular cells, T$_{FH}$ cells, and GC B cells (reduction of each subset by approximately a factor of 5), as well as lower anti-Ova total IgG, IgG1, IgG2c, IgG2b, and IgG3 titers subsequent to Ova-eCFA immunization (Fig 3, *D-G* and data not shown). Intriguingly, the residual anti-Ova IgG1 Abs in IL-6 KO mice did not show the reduced galactosylation and sialylation levels found in WT mice (Fig 3, *H* and see Fig E7, *A-C* in this article's Online Repository at www.jacionline.org). Accordingly, unlike WT mice, IL-6 KO animals failed to downregulate St6gal1 expression in the residual splenic IgG1$^+$ Ova$^+$ GC B cells and PCs following Ova-eCFA immunization on day 14, as well as in BM IgG1$^+$ Ova$^+$ PCs, after recall with Ova, on day 36 (Fig 3, *I*). Similar findings were obtained by applying an anti–IL-6R blocking Ab in Ova-eCFA immunized WT mice (data not shown).

Notably, a comparable effect was observed following immunization of IL-6 KO mice with Ova-IFA or Ova-alum (Fig 3, *J* and *K* and see Fig E7, *A-C*), showing that alum has at least a certain inflammatory potential and implying that the T$_{FH}$-inducing cytokine IL-6 is
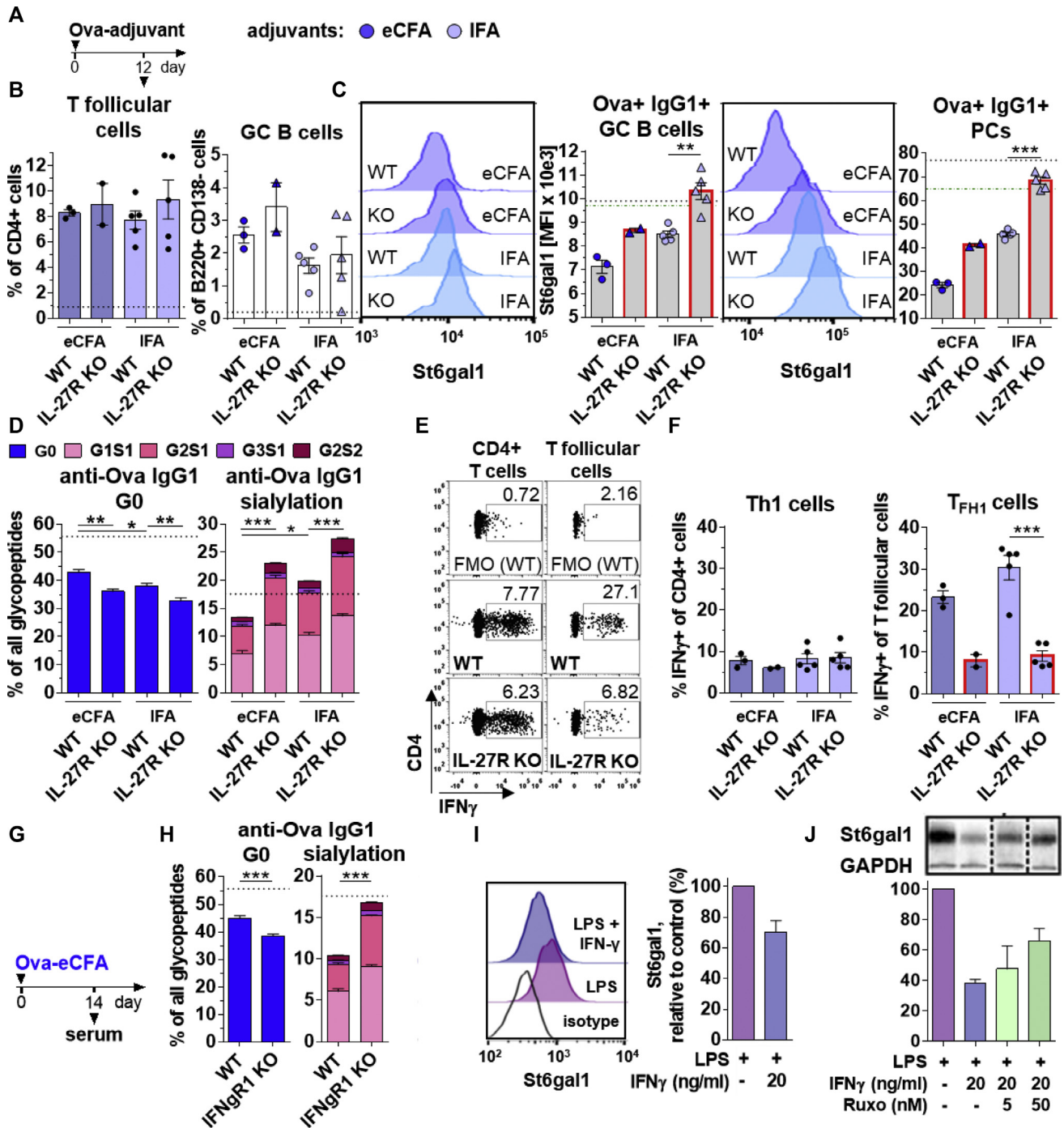
FIG 4. IL-27R signaling is necessary to induce IFN-γ–producing T_{FH1} cells and downregulate St6gal1 expression in GC B cells and PCs, as well as IgG Fc galactosylation and sialylation. **A,** The experimental design for (**B**) to (**F**) was as follows: WT and IL-27R KO mice were immunized with Ova plus eCFA or IFA and analyzed on day 12 (cell analysis, n = 2-5 per group; serum analysis, n = 3-5 per group). **B,** Frequencies of splenic CXCR5+ ICOS+ T follicular and GL7+ FAS+ GC B cells. Horizontal dashed lines indicate average cell population frequencies of untreated mice. **C,** St6gal1 protein expression (median fluorescence intensity [MFI]), including overlay histograms of representative mice, in Ova-specific (Ova+) IgG1+ splenic GC B cells and PCs. Horizontal dashed lines indicate average St6gal1 expression levels in IgG1+ GC B cells and PCs of untreated mice (black indicates WT mice; green indicates IL-27R KO mice). **D,** Serum anti-Ova IgG1 agalactosylation and sialylation. Horizontal dashed lines indicate average bulk IgG1 G0 and sialylation before immunization. **E,** Representative flow cytometry IFN-γ staining (including IFN-γ FMOs) of splenic CD4+ (left) or CXCR5+ ICOS+ CD4+ (right) T follicular cells after immunization with Ova-eCFA. **F,** Frequencies of splenic IFN-γ–producing T_H1 and T_{FH1} cells. **G,** The experimental design for (**H**) was as follows: WT and IFN-γRI KO mice were immunized with Ova-eCFA and analyzed on day 14 (n = 5 per group). **H,** Serum anti-Ova IgG1 agalactosylation and sialylation. **I,** The effect of IFN-γ on St6gal1 protein expression (MFI and flow cytometry) in LPS-induced IgG+ B cells in vitro. The expression is normalized to the LPS-only control. **J,** The effect of IFN-γ and ruxolitinib (Ruxo), a JAK1/2 inhibitor, on St6gal1 protein expression (immunoblotting) in LPS-stimulated B cells in vitro. The expression is normalized to glyceraldehyde-3-phosphate dehydrogenase (GAPDH) and then to the LPS-only control. One of at least 2 independent experiments is shown for each investigation.

crucial for the downregulation of St6gal1 expression and antigen-specific serum IgG galactosylation and sialylation levels.

To further test the scenario in which IL-6 produced by CD11c^{+} dendritic cells (DCs) influences the induction of IgG Fc glycosylation, we analyzed Ova-CFA–induced changes in IgG Fc glycosylation in mice lacking IL-6 in CD11c^{+} DCs (IL-6 fl/fl × CD11c-Cre). In line with the hypothesis, the conditional KO mice showed significantly higher anti-Ova IgG1 sialylation levels and also a trend toward higher IgG2 sialylation levels on day 14 compared with the controls (see Fig E7, *D* and *E*).

The IL-27R is required for induction of IFN-γ–producing T$_{FH1}$ cells and low St6gal1 expression in IgG[+] GC B cells

To further identify T$_{FH}$ subsets responsible for the downregulation of St6gal1 expression in GC B cells, we analyzed the role of the IL-27R, because IL-27 has been reported to induce T$_H$1 responses[31] and contribute to the T follicular cell response subsequent to immunization with water-in-oil adjuvants.[50]

We immunized WT and IL-27R KO (WSX-1 KO) mice with Ova-eCFA or Ova-IFA and analyzed the mice on day 12 (Fig 4, *A*). The IL-27R KO mice showed comparable frequencies of T follicular, T$_{FH}$, and T$_{FR}$ cells as well as GC B-cell and PC subsets compared with WT mice (Fig 4, *B* and see Fig E8 in this article's Online Repository at www.jacionline.org). However, the potential of the 2 water-in-oil adjuvants to downregulate St6gal1 expression in IgG1^{+} Ova[+] GC B cells and PCs as well as serum anti-Ova IgG1 galactosylation and sialylation levels in WT mice was gradually reduced in IL-27R KO mice (Fig 4, *C* and *D* and Fig E8).

Intriguingly, we found that the frequency of IFN-γ–producing T follicular (T$_{FH1}$) cells[49,51,52] was highly reduced in IL-27R KO mice (a trend for eCFA and significant for IFA), whereas the frequency of IFN-γ–producing CD4^{+} T$_H$1 cells was not reduced (Fig 4, *E* and *F*). These results implied a further important mechanism for the downregulation of St6gal1 in IgG[+] GC B cells subsequent to immunization via IL-27R–dependent IFN-γ[+] T$_{FH1}$ cells.

IFN-γ downregulates St6gal1 expression in B cells

IFN-γ signaling in B cells has been reported to play a critical role in the induction of GC B-cell responses in the context of inflammatory (auto)immune diseases.[48,52-55] To further elucidate the potential of IL-27R–dependent T$_{FH1}$ cells, we studied whether IFN-γ may contribute to programming of low St6gal1 expression levels in B cells.

First, we determined that the downregulation of anti-Ova IgG1, as well as IgG2 subclass galactosylation and sialylation levels subsequent to Ova-eCFA immunization, were highly diminished in IFN-γ receptor I–deficient (IFN-γRI KO) mice compared with control WT mice on day 14 (Fig 4, *G* and *H* and see Fig E9, *A* and *B* in this article's Online Repository at www.jacionline.org).

In addition, IFN-γ reduced St6gal1 protein expression in LPS-induced B-cell cultures (Fig 4, *I* and *J*), further confirming a direct effect of IFN-γ on B cells. This IFN-γ effect on St6gal1 protein expression in B cells was sensitive to Ruxolitinib, a JAK1/2 inhibitor (Fig 4, *J*).

These results are in line with a model in which IL-27R–dependent IFN-γ[+] T$_{FH1}$ cells act on GC B cells to downregulate St6gal1 expression.

The effect of Mtb in IFA on St6gal1 expression is linked to an IL-6– and IL-23–dependent induction of T$_{FH}$ and IL-17A^{+} T$_{FH17}$ cells and an increased T$_{FH}$ cell–to–T$_{FR}$ cell ratio

Next, we investigated the potential of Mtb to downregulate IgG Fc galactosylation and sialylation. By using IL-17A reporter mice, we discovered that compared with immunizations using Ova-IFA and Ova-alum alone, addition of Mtb to Ova-IFA (eCFA) clearly enhanced not only the accumulation of IL-17A^{+} T$_H$17 cells but also the accumulation of IL-17A[+] T$_{FH17}$ cells[56-58] on day 12 (Fig 5, *A* and *B*).

To study the impact of the potential IL-23–T$_H$17/T$_{FH17}$ axis on the Ova-eCFA–induced GC response and IgG Fc glycosylation pattern, we analyzed IL-23p19 KO mice in comparison with WT and IL-6 KO mice following immunization with Ova-eCFA on day 14. Not only IL-6 KO mice but also IL-23p19 KO mice showed significantly reduced T follicular and T$_{FH}$ cell frequencies as well as T$_{FH}$ cell–to–T$_{FR}$ cell ratios (Fig 5, *C* and *D*). Furthermore, IL-6 KO mice as well as IL-23p19 KO mice showed a strong reduction of T$_{FH17}$ cells (Fig 5, *D*). Notably, the residual T follicular cells in IL-23p19 KO mice, as well as those in IL-6 KO mice, showed no reduction in the percentages of T$_{FH1}$ cells subsequent to immunization (data not shown).

Compared with the phenotypes of WT mice, the phenotypes of both KO mouse strains were associated with significantly reduced frequencies of GC B cells and enhanced St6gal1 expression levels (significant for IL-6 KO and a trend for IL-23p19 KO mice) in antigen-specific IgG1^{+} GC B cells and PCs (Fig 5, *E* and *F* and data not shown). Accordingly, anti-Ova IgG1 Fc sialylation was significantly enhanced in IL-23p19 KO mice following Ova-eCFA immunization compared with in WT mice, even though not as strongly as in IL-6 KO mice (Fig 5, *G*), probably because of the overlapping IFA-dependent IL-6 effect. Tending or significantly enhanced St6gal1 expression or anti-Ova IgG1 Fc sialylation levels could also be seen in the IL-17A KO mice following Ova-eCFA immunization compared with in WT mice (Fig 5, *H* and *I* and see Fig E9, *C* and *D*).

Mtb and its cord factor also downregulate St6gal1 expression when added to alum

Next, we investigated whether Mtb could also downregulate IgG Fc galactosylation and sialylation levels when added to Ova-alum and whether the effect of Mtb could be restricted to a single Mtb surface molecule. We found that compared with immunizations using Ova-alum alone, immunizations using Ova-alum with Mtb, as well as those using Ova-alum with the synthetic analog of its Mincle receptor-binding cord factor trehalose 6,6'-dimycolate (ie, TDB), significantly enhanced the frequencies of T follicular, T$_{FH}$, T$_{FH17}$, and GC B cells and the T$_{FH}$ cell–to–T$_{FR}$ cell ratio and also reduced the St6gal1 expression (significant for Ova-alum plus Mtb and a trend for Ova-alum plus TDB) in GC B cells on day 12 (Fig 5, *J-L* and see Fig E10 in this article's Online Repository at www.jacionline.org). Furthermore, compared with immunizations using Ova-alum or Ova-TDB alone, immunizations using Ova-alum plus Mtb or TDB significantly reduced the serum anti-Ova IgG1 galactosylation and sialylation levels on days 12 and 14 (Fig 5, *M* and see Fig E10).

Together, these data indicated that the effect of Mtb in IFA on enhancement of the frequencies of T$_{FH}$ and T$_{FH17}$ cells, as well
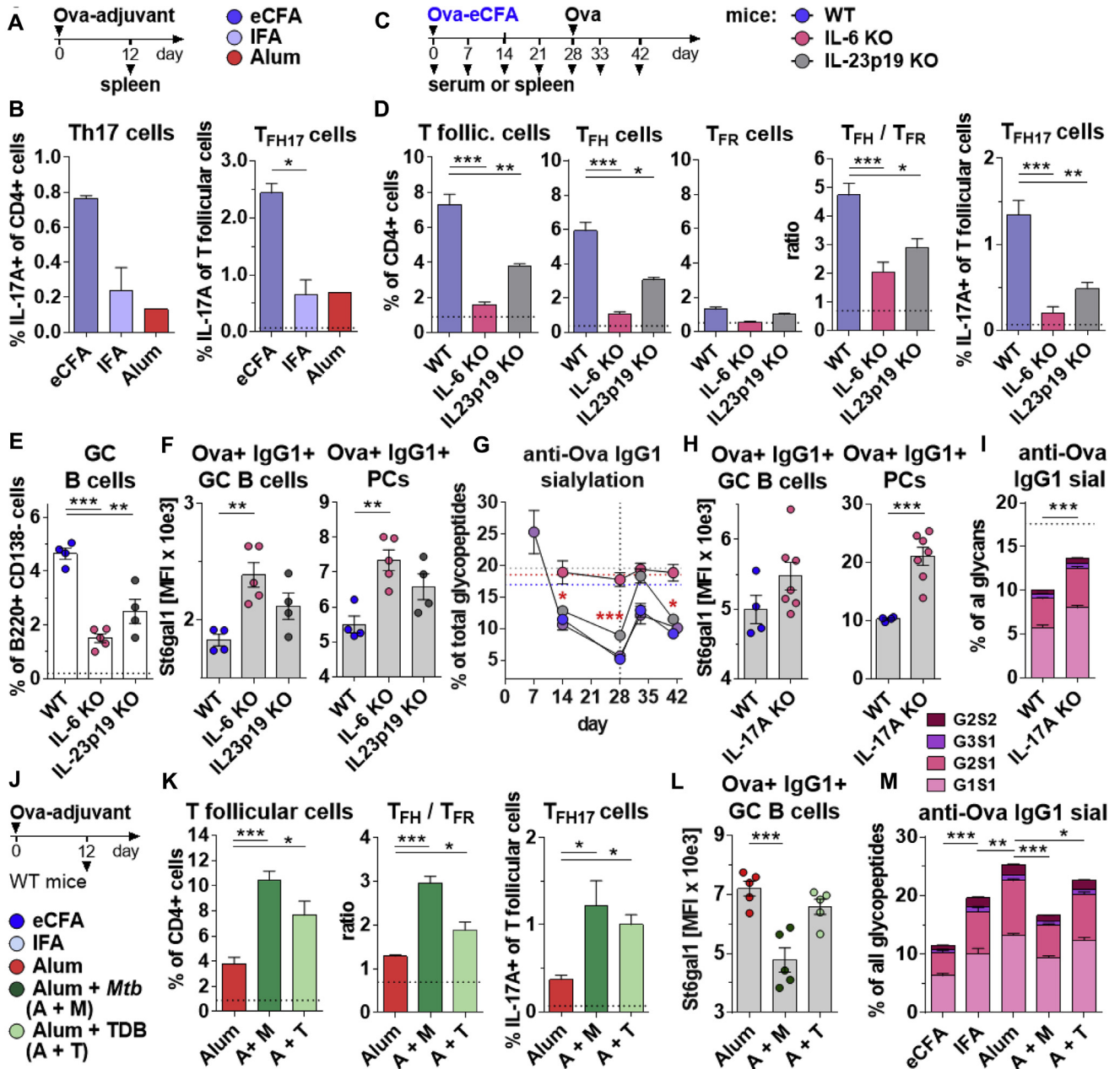
FIG 5. Mtb or TDB combined with IFA or alum induce IL-6– and IL-23p19–dependent T follicular and T_{FH17} cells, increase the T_{FH} cell–to–T_{FR} cell ratio, and downregulate St6gal1 protein expression in GC B cells. **A,** The experimental design for (**B**) was as follows: IL-17A–EGFP reporter mice were immunized with Ova plus eCFA, IFA, or alum and analyzed on day 12 (n = 2-5 per group). **B,** Frequencies of splenic T_H17 cells and T_{FH17} cells. **C,** The experimental design for (**D**) to (**G**) was as follows: WT, IL-6 KO, and IL-23p19 KO female mice were immunized with Ova-eCFA and boosted with Ova without adjuvant on day 28 (n = 4 or 5 per group). **D** and **E,** Frequencies of T follicular, T_{FH}, T_{FR}, and T_{FH17} cells and the T_{FH} cell–to–T_{FR} cell ratio and frequencies of GL7$^+$ FAS$^+$ GC B cells on day 14. Horizontal dashed lines indicate average cell population frequencies of untreated mice. **F,** St6gal1 protein expression in Ova-specific (Ova$^+$) IgG1$^+$ GC B cells and PCs on day 14. **G,** Serum anti-Ova IgG1 Fc sialylation (G1S1 + G2S1 + G3S1 + G2S2) on the indicated time points (the WT data from Fig 1, E (purple) are shown for comparison). Horizontal dashed lines indicate average bulk IgG1 glycosylation before immunization. Asterisks indicate the significant differences between the WT and the IL-23p19 KO data on the indicated time points. **H** and **I,** WT and IL-17A KO mice were immunized with Ova-eCFA (n = 4-7 per group). St6gal1 protein expression in Ova$^+$ IgG1$^+$ GC B cells and PCs and serum anti-Ova IgG1 Fc sialylation (sial) on day 14. The horizontal dashed line indicates average bulk IgG1 sialylation before immunization. **J,** The experimental design for (**K**) to (**M**) was as follows: WT female mice were immunized with Ova plus eCFA, IFA, alum, alum + Mtb, or alum + TDB (TDB-HS15) and analyzed on day 12 (n = 5 per group). **K,** Frequencies of splenic T follicular cells and T_{FH17} cells and the T_{FH} cell–to–T_{FR} cell ratios. **L,** St6gal1 protein expression in Ova$^+$ IgG1$^+$ splenic GC B cells. **M,** Serum anti-Ova IgG1 Fc sialylation. One of 2 independent experiments is shown for each set of investigations.

as on the T_{FH} cell–to–T_{FR} cell ratio and on the downregulation of the anti-Ova IgG galactosylation and sialylation levels, could also be found when Mtb or its cord factor analog was added to alum.

The potential of the costimulus determines the IgG1$^+$ GC B-cell transcriptome

To investigate whether different costimuli during immunization in general affect the IgG$^+$ GC B-cell phenotype and to explore the molecular pathways responsible for setting St6gal1 expression in IgG-producing cells, we compared the transcriptomes of Ova-eCFA– and Ova-LPS–induced splenic IgG1$^+$ GC B cells sorted on day 8 (Fig 6, *A* and see Fig E11 in this article's Online Repository at www.jacionline.org).

We revealed distinct transcriptional signatures between Ova-eCFA– and Ova-LPS–induced IgG1$^+$ GC B cells (Fig 6 and see Fig E11). First, the St6gal1 transcript was upregulated in Ova-LPS–induced IgG1$^+$ GC B cells compared with in the Ova-eCFA group (Fig 6, *C*). Further, the Ova-eCFA immunization induced the expression of many genes related to inflammatory signaling pathways (Fig 6, *C* and *D* and see Fig E11). Notably, gene set enrichment analyses revealed that IFN-γ–responsive genes were overrepresented among the transcripts upregulated in Ova-eCFA–induced IgG1$^+$ GC B cells (Fig 6 and see Fig E11) confirming our findings already described.

The data further indicated that immunizations with different adjuvants induce distinct GC B-cell responses, including the differential expression of St6gal1.

DISCUSSION

In this study, we discovered that different adjuvants induce distinct GC responses, resulting in IgG$^+$ GC B cells with distinct transcriptomes and St6gal1 expression levels corresponding to the induced IgG Fc glycosylation patterns. Overall, low St6gal1 expression in GC B cells and low IgG Fc galactosylation and sialylation levels were highly dependent on the T_{FH}-inducing cytokine IL-6 (here in particular, induced with water-in-oil adjuvants and Mtb). Furthermore, we identified an IL-27R–dependent IFN-γ$^+$ T_{FH1} cell-linked mechanism and an IL-6– and IL-23–dependent IL-17A$^+$ T_{FH17} cell– and T_{FH} cell–to–T_{FR} cell ratio–linked mechanism that downregulates St6gal1 expression in antigen-specific IgG$^+$ GC B cells as well as IgG Fc galactosylation and sialylation levels. The latter 2 effects can be induced by Mtb and its identified cord factor. The T_H2 cell adjuvants alum, Adju-Phos, and AddaVax,[59] as well as the TLR ligands LPS, MPLA, R848, and Poly (I:C), induced a much lower downregulation of IgG Fc galactosylation and sialylation.

In the past, T_H1 and T_H17 cell, but not T_H2 cell, immune responses have been associated with protective immune responses against different pathogens subsequent to vaccination.[59] In addition, T_H1 cell and IL-23/T_H17 cell immune responses have been linked to the induction of IgG Abs with low galactosylation and sialylation levels.[11,16] Here, we discovered and analyzed corresponding IL-27R–dependent T_{FH1} and IL-6/IL-23–dependent T_{FH17} cell immune responses in the GC and their influence on the St6gal1 expression in GC B cells and the IgG Fc galactosylation and sialylation levels.

The GC reaction is a prerequisite for generation of highly hypermutated IgG$^+$ long-lived PCs and memory B cells.[2] Although we could not distinguish between GC-derived and non–GC-derived antigen-specific IgG$^+$ PCs or IgG Abs at the different time points, our data strongly indicate that GC-derived PCs produce the GC-programmed IgG Ab glycosylation pattern subsequent to the primary immunization. Notably, recent studies have shown that more than 80% of antigen-specific CD138$^+$ PCs derive from GC B cells after immunization with a foreign protein antigen plus CFA on day 15.[4]

Further, we observed similar dynamics of serum anti-Ova IgG Fc glycosylation after antigen reexposure without adjuvant on day 28. On day 33, the IgG Fc galactosylation and sialylation levels transiently increased once again in all groups as observed on day 7, suggesting a fast extrafollicular PC response by newly activated and/or (in particular) reactivated memory B cells.[3] On day 42 and 57, however, anti-Ova IgG Ab galactosylation and sialylation levels decreased again and showed comparable differences between the groups, as observed between day 14 and 28 before the boost.

Accordingly, we were able to observe corresponding differences in St6gal1 protein expression in BM PCs after the boost on day 36. Considering that those BM PCs may contain long-lived PCs that can survive over several years,[2] we were able to speculate that differences in St6gal1 expression and antigen-specific IgG sialylation levels may be fixed after the primary immunization and may be stable for a longer period of time.

However, future studies, also for a longer period of time (eg, with inducible reporter mice, in which GC-derived PCs and memory B cells can be specifically tracked[4]) will give an insight into the stability of St6gal1 expression and the lifespan of GC-derived and non–GC-derived PCs and memory B cells induced after the primary immunization or after boosting with the same, a different, or no adjuvant. Such studies might also clarify whether potentially epigenetically fixed St6gal1 expression could be redirected in long-lived PCs and memory B cells, which could also be highly interesting for the treatment of autoimmunity.

Our IL-6 data are in accordance with the findings of recent genome-wide association studies showing that IL-6 signaling (SNPs in the IL6ST [gp130] gene) correlates with low serum bulk IgG galactosylation and sialylation levels in humans.[60] Furthermore, IL-6 has been linked to strong T_{FH} cell responses (eg, after immunization with water-in-oil adjuvants).[45] IL-6 might thereby be produced by DCs, macrophages, and/or B cells to drive the T_{FH} cell response.[34,48,61,62] Although, we cannot exclude additional effects of IL-6 (eg, on PC survival), our data clearly showed an effect of IL-6 on the number of T_{FH} cells associated with the number of antigen-specific IgG$^+$ GC B cells and their St6gal1 expression. Therapeutic anti–IL-6 or anti–IL-6R blocking Abs in the treatment of inflammatory autoimmune diseases might have similar effects.

In addition, we discovered that IL-27R–dependent IFN-γ$^+$ T_{FH1} cells are linked to the effect of the water-in-oil adjuvant IFA on St6gal1 expression and IgG Fc galactosylation and sialylation levels. Furthermore, we were able to determine that IgG1 and IgG2 galactosylation and sialylation levels were enhanced in IFN-γRI KO mice compared with in control WT mice subsequent to immunization with Ova-eCFA, confirming our previous studies of serum anti-Ova total IgG glycan analysis after Ova-CFA immunization.[11] Intriguingly, deletion of the IFN-γRI influenced not only the glycosylation pattern of the IgG2 subclasses containing the IFN-γ–dependent IgG2c but also that of the IgG1 subclass. Furthermore, we observed that IFN-γ could downregulate St6gal1 expression in cultured B cells via the JAK1/2 signaling pathway.
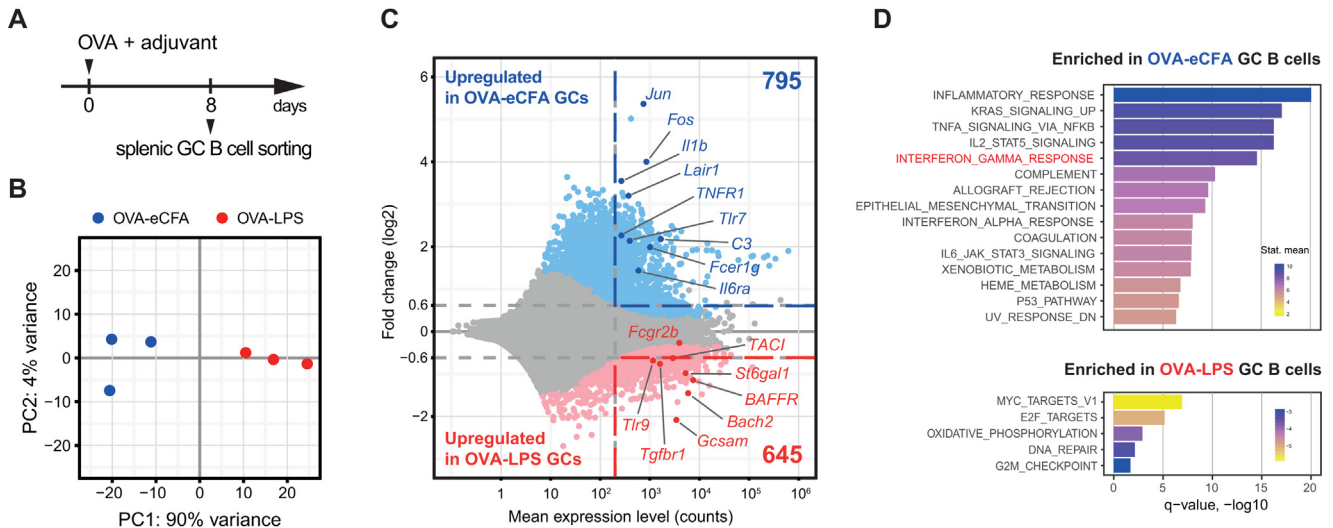
FIG 6. Adjuvants regulate the IgG1$^+$ GC B-cell transcriptome, including IFN-γ–responsive genes and St6gal1. **A,** The experimental design was as follows: WT mice were immunized with Ova-eCFA or Ova-LPS (n = 3). On day 8, spleens were prepared for flow cytometry sorting of IgG1$^+$IgM$^-$ (B220$^+$CD138$^-$GL7$^+$FAS$^+$) GC B cells and subsequent RNA purification. **B,** A principal component analysis (PCA) plot of Ova-eCFA– and Ova-LPS–induced GC B-cell transcriptomes. The principal components were calculated by using the 500 genes with the highest variance. Each symbol represents an individual mouse. **C,** A counts-versus–fold change "minus-average" plot showing differential gene expression. Genes that were significantly upregulated (adjusted *P* value < .05) in Ova-eCFA– or Ova-LPS–induced IgG1$^+$ GC B cells are shown in light blue or light red, respectively. Genes that met 2 criteria, namely, mean normalized counts greater than 200 and a log2 fold change of greater than 0.6 or less than or equal to 0.6, are shown in dashed blue or red boxes, respectively. **D,** Gene set enrichment results showing the hallmark gene sets significantly enriched (*q* value [ie, Benjamini-Hochberg adjusted *P* value] < 0.05) in IgG1$^+$ GC B cells. The absolute value of the statistical mean represents the magnitude of gene set–level changes, and its sign indicates direction of the changes.

These findings are in line with recent observations that IL-27 is important for initial IFN-γ$^+$ CD4$^+$ T-cell responses[31] and that IFN-γ can force inflammatory (auto)immune GC B-cell responses.[52-55]

These data led to the suggestion that protective T$_H$1 immune responses following vaccination[59] might be mediated at least in part by IL-27R–dependent IFN-γ$^+$ T$_{FH1}$ cells and their influence on the IgG Fc glycosylation pattern. Various new adjuvants connected to T$_H$1 immune responses[59] might induce this effect. Accordingly, such T$_{FH1}$ immune responses might be involved in the development of inflammatory autoimmune diseases.

Further, we identified an effect of Mtb in IFA and alum on the induction of IgG$^+$ GC B cells with reduced St6gal1 expression levels. This effect was dependent on IL-6 as well as on IL-23, and it was linked to the induction of T$_{FH}$ and IL-17A$^+$ T$_{FH17}$ cells as well as to an increased T$_{FH}$ cell–to–T$_{FR}$ cell ratio. Furthermore, the effect of Mtb in alum could be restricted to its Mincle-binding cord factor analog TDB.[59,63]

These findings are in agreement with those of studies, which showed that IL-6 programs T$_H$17 cell differentiation[64] by promoting the IL-23 pathway[16,65] and that a new adjuvant containing a synthetic analog of the cord factor (TDB) in liposomes is inducing T$_H$17 cells.[59] TDB has been described as interacting with the Mincle receptor to activate antigen-presenting cells via its signaling subunit, the FcRγ-chain, containing an ITAM motif. This activation results in the phosphorylation of Syk to influence the priming of naive CD4$^+$ T cells.[59,63]

Although corresponding differences in anti-Ova IgG1 Fc sialylation could be observed in IL-17A KO mice, no significant differences were observed in mice deficient for IL-22, which is a described mediator of inflammatory T$_H$17 cells.[22] Effects of IL-17A, but also of further effector molecules of T$_{FH17}$ cells[66] might contribute to downregulation of the St6gal1 expression in GC B cells.

Mtb or its cord factor in IFA or alum also induced an increased T$_{FH}$ cell–to–T$_{FR}$ cell ratio. The T$_{FH}$ cell–driven response is counteracted by T$_{FR}$ cells, which can influence the T$_{FH}$ cells as well as the GC B cells.[43,44] Inhibitory molecules of T$_{FR}$ cells such as CTLA-4 might mediate inhibitory effects.[44] These observations further indicate the important role of the GC response for the antigen-specific serum IgG Fc glycosylation pattern.

In the future, it will be critical to explore the role of the molecular signaling axes of IL-6, IL-27, IFN-γ, IL-23, and IL-17, and as well as T$_{FR}$ cells in more detail by also using further cell-specific conditional gene targeting approaches.

The immunization protocols that we used in this study resemble vaccination strategies intended to induce protective immune responses. These findings may therefore have important implications for development of more efficient protocols for human vaccination. Thus far, the success of vaccination protocols has commonly been verified by the induction and persistence of serum IgG Ab titers. However, discovering mechanisms that regulate not only amounts but also functional properties of IgG Abs would significantly improve our understanding of immune responses for developing novel vaccination strategies.[1,17]

Even though early sialylated IgG Abs have been described as being powerful in delivering the antigen to the GC,[14,41] late pathogenic IgG Abs might need the same properties as pathogenic IgG autoantibodies in inflammatory autoimmune diseases. Recently, specific IgG Abs with reduced galactosylation and sialylation levels have been linked to protection in HIV controllers (infected

individuals without HIV enrichment)[23] and to improved protection of rhesus macaques against simian immunodeficiency virus after vaccination with different adjuvants.[24] Understanding mechanisms that reduce antigen-specific IgG galactosylation and sialylation levels during the GC response might help in developing vaccines with high protection. A correlation between success of vaccination and the induction of T_H1 and T_H17 cells following vaccination has already been suggested.[59] Here, we have further shown the importance of such subsets in the GC response after immunization for the induction of low St6gal1 expression in IgG^+ GC B cells and low IgG galactosylation and sialylation levels. In the future, the role of our findings for vaccine-induced protection against infections need to be elaborated in humans also.

Finally, our GC B-cell transcriptome data indicate that the nature of the costimulus during immune responses programs further B-cell functions well beyond IgG Fc glycosylation. Ova-eCFA–induced $IgG1^+$ GC B cells revealed a proinflammatory transcriptional signature, including many genes that regulate cell lifespan, migration, and cytokine expression. Some of these genes might be used as markers to distinguish B-cell subsets that program different types of IgG glycosylation, which could be promising tools to verify immune responses during infection and vaccination. Although we found no enhanced transcription of the B4galt1 gene after Ova-LPS immunization, our data suggest that IgG Fc galactosylation is also regulated in antigen-specific IgG^+ GC B cells. Posttranscriptional modifications might regulate the B4galt1 protein expression or function. Unfortunately, we were not able to establish a reliable B4galt1 protein staining.

In summary, our data showed that immunizations with different adjuvants induce distinct GC responses and suggest a model in which, overall, IL-6–induced T_{FH} cells (in particular, those induced by water-in-oil adjuvants) downregulate the St6gal1 expression in GC B cells subsequent to immunization. Further, we identified an IL-27R–dependent IFN-γ^+ T_{FH1} cell–mediated and an IL-6– and IL-23–dependent IL-17A$^+$ T_{FH17} cell– and T_{FH} cell–to–T_{FR} cell ratio–mediated effect of T_H1 and T_H17 cell adjuvants, respectively, on the St6gal1 expression in GC B cells and on the IgG Fc galactosylation and sialylation levels.

Key messages

- **Protein antigens in combination with different adjuvants induce distinct IgG Fc glycosylation patterns by programming the germinal center reaction.**

- **Overall, IL-6–dependent T_{FH} cells—here in particular induced by water-in-oil adjuvants and *Mycobacterium tuberculosis*—are necessary to program low IgG sialylation levels in GC B cells.**

- **Adjuvants that induce IL-27R–dependent IFN-γ^+ T_{FH1} cells, IL-6/IL-23–dependent IL-17A$^+$ T_{FH17} cells, and high T_{FH} cell–to–T_{FR} cell ratios further program low IgG sialylation.**

REFERENCES

1. Alter G, Ottenhoff THM, Joosten SA. Antibody glycosylation in inflammation, disease and vaccination. Semin Immunol 2018;39:102-10.
2. Manz RA, Thiel A, Radbruch A. Lifetime of plasma cells in the bone marrow. Nature 1997;388:133-4.
3. Inoue T, Moran I, Shinnakasu R, Phan TG, Kurosaki T. Generation of memory B cells and their reactivation. Immunol Rev 2018;283:138-49.
4. Ise W, Fujii K, Shiroguchi K, Ito A, Kometani K, Takeda K, et al. T follicular helper cell-germinal center B cell interaction strength regulates entry into plasma cell or recycling germinal center cell fate. Immunity 2018;48:702-15.e4.
5. Ise W, Kurosaki T. Plasma cell differentiation during the germinal center reaction. Immunol Rev 2019;288:64-74.
6. Nimmerjahn F, Ravetch JV. Divergent immunoglobulin g subclass activity through selective Fc receptor binding. Science 2005;310:1510-2.
7. Kaneko Y, Nimmerjahn F, Ravetch JV. Anti-inflammatory activity of immunoglobulin G resulting from Fc sialylation. Science 2006;313:670-3.
8. Anthony RM, Kobayashi T, Wermeling F, Ravetch JV. Intravenous gammaglobulin suppresses inflammation through a novel T(H)2 pathway. Nature 2011;475:110-3.
9. Oefner CM, Winkler A, Hess C, Lorenz AK, Holecska V, Huxdorf M, et al. Tolerance induction with T cell-dependent protein antigens induces regulatory sialylated IgGs. J Allergy Clin Immunol 2012;129:1647-55.e13.
10. Karsten CM, Pandey MK, Figge J, Kilchenstein R, Taylor PR, Rosas M, et al. Anti-inflammatory activity of IgG1 mediated by Fc galactosylation and association of FcγRIIB and dectin-1. Nat Med 2012;18:1401-6.
11. Hess C, Winkler A, Lorenz AK, Holecska V, Blanchard V, Eiglmeier S, et al. T cell-independent B cell activation induces immunosuppressive sialylated IgG antibodies. J Clin Invest 2013;123:3788-96.
12. Collin M, Ehlers M. The carbohydrate switch between pathogenic and immunosuppressive antigen-specific antibodies. Exp Dermatol 2013;22:511-4.
13. Pincetic A, Bournazos S, DiLillo DJ, Maamary J, Wang TT, Dahan R, et al. Type I and type II Fc receptors regulate innate and adaptive immunity. Nat Immunol 2014;15:707-16.
14. Wang TT, Maamary J, Tan GS, Bournazos S, Davis CW, Krammer F, et al. Anti-HA glycoforms drive B cell affinity selection and determine influenza vaccine efficacy. Cell 2015;162:160-9.
15. Ohmi Y, Ise W, Harazono A, Takakura D, Fukuyama H, Baba Y, et al. Sialylation converts arthritogenic IgG into inhibitors of collagen-induced arthritis. Nat Commun 2016;7:11205.
16. Pfeifle R, Rothe T, Ipseiz N, Scherer HU, Culemann S, Harre U, et al. Regulation of autoantibody activity by the IL-23-TH17 axis determines the onset of autoimmune disease. Nat Immunol 2017;18:104-13.
17. Jennewein MF, Alter G. The immunoregulatory roles of antibody glycosylation. Trends Immunol 2017.
18. Epp A, Hobusch J, Bartsch YC, Petry J, Lilienthal GM, Koeleman CAM, et al. Sialylation of IgG antibodies inhibits IgG-mediated allergic reactions. J Allergy Clin Immunol 2018;141:399-402.e8.
19. Lilienthal GM, Rahmöller J, Petry J, Bartsch YC, Leliavski A, Ehlers M. Potential of murine IgG1 and human IgG4 to inhibit the classical complement and Fcγ receptor activation pathways. Front Immunol 2018;9:958.
20. Bartsch YC, Rahmöller J, Mertes MMM, Eiglmeier S, Lorenz FKM, Stoehr AD, et al. Sialylated autoantigen-reactive IgG antibodies attenuate disease development in autoimmune mouse models of lupus nephritis and rheumatoid arthritis. Front Immunol 2018;9:1183.
21. Pagan JD, Kitaoka M, Anthony RM. Engineered sialylation of pathogenic antibodies in vivo attenuates autoimmune disease. Cell 2018;172:564-77.e13.
22. Zheng Y, Danilenko DM, Valdez P, Kasman I, Eastham-Anderson J, Wu J, et al. Interleukin-22, a T(H)17 cytokine, mediates IL-23-induced dermal inflammation and acanthosis. Nature 2007;445:648-51.
23. Ackerman ME, Crispin M, Yu X, Baruah K, Boesch AW, Harvey DJ, et al. Natural variation in Fc glycosylation of HIV-specific antibodies impacts antiviral activity. J Clin Invest 2013;123:2183-92.
24. Vaccari M, Gordon SN, Fourati S, Schifanella L, Liyanage NP, Cameron M, et al. Adjuvant-dependent innate and adaptive immune signatures of risk of SIVmac251 acquisition. Nat Med 2016;22:762-70.
25. Mahan AE, Jennewein MF, Suscovich T, Dionne K, Tedesco J, Chung AW, et al. Antigen-specific antibody glycosylation is regulated via vaccination. PLoS Pathog 2016;12:e1005456.
26. Kao D, Lux A, Schaffert A, Lang R, Altmann F, Nimmerjahn F. IgG subclass and vaccination stimulus determine changes in antigen specific antibody glycosylation in mice. Eur J Immunol 2017;47:2070-9.

27. Huang S, Hendriks W, Althage A, Hemmi S, Bluethmann H, Kamijo R, et al. Immune response in mice that lack the interferon-gamma receptor. Science 1993;259: 1742-5.

28. Kopf M, Baumann H, Freer G, Freudenberg M, Lamers M, Kishimoto T, et al. Impaired immune and acute-phase responses in interleukin-6-deficient mice. Nature 1994;368:339-42.

29. Nakae S, Komiyama Y, Nambu A, Sudo K, Iwase M, Homma I, et al. Antigen-specific T cell sensitization is impaired in IL-17-deficient mice, causing suppression of allergic cellular and humoral responses. Immunity 2002;17:375-87.

30. Ghilardi N, Kljavin N, Chen Q, Lucas S, Gurney AL, De Sauvage FJ. Compromised humoral and delayed-type hypersensitivity responses in IL-23-deficient mice. J Immunol 2004;172:2827-33.

31. Yoshida H, Hamano S, Senaldi G, Covey T, Faggioni R, Mu S, et al. WSX-1 is required for the initiation of Th1 responses and resistance to L. major infection. Immunity 2001;15:569-78.

32. Price AE, Reinhardt RL, Liang HE, Locksley RM. Marking and quantifying IL-17A-producing cells in vivo. PLoS One 2012;7:e39750.

33. Quintana A, Erta M, Ferrer B, Comes G, Giralt M, Hidalgo J. Astrocyte-specific deficiency of interleukin-6 and its receptor reveal specific roles in survival, body weight and behavior. Brain Behav Immun 2013;27:162-73.

34. Heink S, Yogev N, Garbers C, Herwerth M, Aly L, Gasperi C, et al. Trans-presentation of IL-6 by dendritic cells is required for the priming of pathogenic TH17 cells. Nat Immunol 2017;18:74-85.

35. de Haan N, Reiding KR, Krištić J, Hipgrave Ederveen AL, Lauc G, Wuhrer M. The N-glycosylation of mouse immunoglobulin G (IgG)-fragment crystallizable differs between IgG subclasses and strains. Front Immunol 2017;8:608.

36. Liao Y, Smyth GK, Shi W. featureCounts: an efficient general purpose program for assigning sequence reads to genomic features. Bioinformatics 2014;30:923-30.

37. Hansen KD, Irizarry RA, Wu Z. Removing technical variability in RNA-seq data using conditional quantile normalization. Biostatistics 2012;13:204-16.

38. Love MI, Huber W, Anders S. Moderated estimation of fold change and dispersion for RNA-seq data with DESeq2. Genome Biol 2014;15:550.

39. Luo W, Friedman MS, Shedden K, Hankenson KD, Woolf PJ. GAGE: generally applicable gene set enrichment for pathway analysis. BMC Bioinformatics 2009; 10:161.

40. Liberzon A, Birger C, Thorvaldsdóttir H, Ghandi M, Mesirov JP, Tamayo P. The Molecular Signatures Database (MSigDB) hallmark gene set collection. Cell Syst 2015;1:417-25.

41. Lofano G, Gorman MJ, Yousif AS, Yu WH, Fox JM, Dugast AS, et al. Antigen-specific antibody Fc glycosylation enhances humoral immunity via the recruitment of complement. Sci Immunol 2018;3.

42. Vaeth M, Schliesser U, Müller G, Reissig S, Satoh K, Tuettenberg A, et al. Dependence on nuclear factor of activated T-cells (NFAT) levels discriminates conventional T cells from Foxp3+ regulatory T cells. Proc Natl Acad Sci U S A 2012; 109:16258-63.

43. Vaeth M, Müller G, Stauss D, Dietz L, Klein-Hessling S, Serfling E, et al. Follicular regulatory T cells control humoral autoimmunity via NFAT2-regulated CXCR5 expression. J Exp Med 2014;211:545-61.

44. Sage PT, Sharpe AH. T follicular regulatory cells. Immunol Rev 2016;271:246-59.

45. Riteau N, Radtke AJ, Shenderov K, Mittereder L, Oland SD, Hieny S, et al. Water-in-oil-only adjuvants selectively promote T follicular helper cell polarization through a type I IFN and IL-6-dependent pathway. J Immunol 2016;197:3884-93.

46. Vinuesa CG, Linterman MA, Yu D, MacLennan IC. Follicular helper T cells. Annu Rev Immunol 2016;34:335-68.

47. Weinstein JS, Herman EI, Lainez B, Licona-Limón P, Esplugues E, Flavell R, et al. TFH cells progressively differentiate to regulate the germinal center response. Nat Immunol 2016;17:1197-205.

48. Arkatkar T, Du SW, Jacobs HM, Dam EM, Hou B, Buckner JH, et al. B cell-derived IL-6 initiates spontaneous germinal center formation during systemic autoimmunity. J Exp Med 2017;214:3207-17.

49. Velu V, Mylvaganam G, Ibegbu C, Amara RR. Tfh1 cells in germinal centers during chronic HIV/SIV infection. Front Immunol 2018;9:1272.

50. Batten M, Ramamoorthi N, Kljavin NM, Ma CS, Cox JH, Dengler HS, et al. IL-27 supports germinal center function by enhancing IL-21 production and the function of T follicular helper cells. J Exp Med 2010;207:2895-906.

51. Reinhardt RL, Liang HE, Locksley RM. Cytokine-secreting follicular T cells shape the antibody repertoire. Nat Immunol 2009;10:385-93.

52. Lüthje K, Kallies A, Shimohakamada Y, Belz GT, Light A, Tarlinton DM, et al. The development and fate of follicular helper T cells defined by an IL-21 reporter mouse. Nat Immunol 2012;13:491-8.

53. Lee SK, Silva DG, Martin JL, Pratama A, Hu X, Chang PP, et al. Interferon-γ excess leads to pathogenic accumulation of follicular helper T cells and germinal centers. Immunity 2012;37:880-92.

54. Domeier PP, Chodisetti SB, Soni C, Schell SL, Elias MJ, Wong EB, et al. IFN-γ receptor and STAT1 signaling in B cells are central to spontaneous germinal center formation and autoimmunity. J Exp Med 2016;213:715-32.

55. Jackson SW, Jacobs HM, Arkatkar T, Dam EM, Scharping NE, Kolhatkar NS, et al. B cell IFN-γ receptor signaling promotes autoimmune germinal centers via cell-intrinsic induction of BCL-6. J Exp Med 2016;213:733-50.

56. Ding Y, Li J, Wu Q, Yang P, Luo B, Xie S, et al. IL-17RA is essential for optimal localization of follicular Th cells in the germinal center light zone to promote autoantibody-producing B cells. J Immunol 2013;191:1614-24.

57. Hsu HC, Yang P, Wang J, Wu Q, Myers R, Chen J, et al. Interleukin 17-producing T helper cells and interleukin 17 orchestrate autoreactive germinal center development in autoimmune BXD2 mice. Nat Immunol 2008;9:166-75.

58. Song W, Craft J. T follicular helper cell heterogeneity: time, space, and function. Immunol Rev 2019;288:85-96.

59. Knudsen NP, Olsen A, Buonsanti C, Follmann F, Zhang Y, Coler RN, et al. Different human vaccine adjuvants promote distinct antigen-independent immunological signatures tailored to different pathogens. Sci Rep 2016;6:19570.

60. Lauc G, Huffman JE, Pučić M, Zgaga L, Adamczyk B, Mužinić A, et al. Loci associated with N-glycosylation of human immunoglobulin G show pleiotropy with autoimmune diseases and haematological cancers. PLoS Genet 2013;9: e1003225.

61. Barr TA, Shen P, Brown S, Lampropoulou V, Roch T, Lawrie S, et al. B cell depletion therapy ameliorates autoimmune disease through ablation of IL-6-producing B cells. J Exp Med 2012;209:1001-10.

62. Garbers C, Heink S, Korn T, Rose-John S. Interleukin-6: designing specific therapeutics for a complex cytokine. Nat Rev Drug Discov 2018;17: 395-412.

63. Shenderov K, Barber DL, Mayer-Barber KD, Gurcha SS, Jankovic D, Feng CG, et al. Cord factor and peptidoglycan recapitulate the Th17-promoting adjuvant activity of mycobacteria through mincle/CARD9 signaling and the inflammasome. J Immunol 2013;190:5722-30.

64. Jones GW, McLoughlin RM, Hammond VJ, Parker CR, Williams JD, Malhotra R, et al. Loss of CD4+ T cell IL-6R expression during inflammation underlines a role for IL-6 trans signaling in the local maintenance of Th17 cells. J Immunol 2010; 184:2130-9.

65. Zhou L, Ivanov II, Spolski R, Min R, Shenderov K, Egawa T, et al. IL-6 programs T(H)-17 cell differentiation by promoting sequential engagement of the IL-21 and IL-23 pathways. Nat Immunol 2007;8:967-74.

66. Kurata I, Matsumoto I, Ohyama A, Osada A, Ebe H, Kawaguchi H, et al. Potential involvement of OX40 in the regulation of autoantibody sialylation in arthritis. Ann Rheum Dis 2019;78:1488-96.
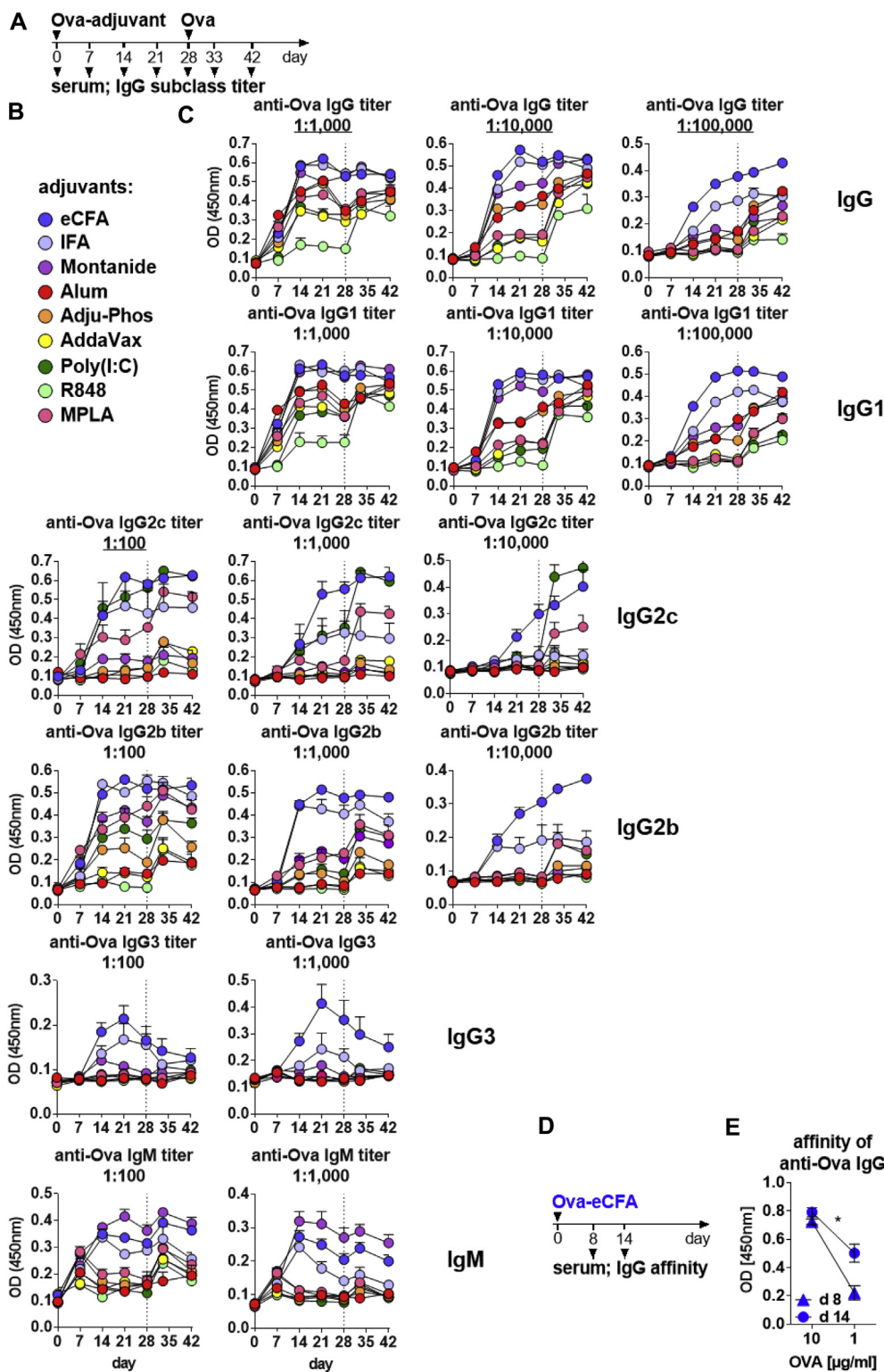
FIG E1. Adjuvants induce distinct IgG subclass titers after immunization with a foreign protein antigen and increased affinity of serum anti-Ova IgG Abs between day 8 and day 14 after Ova-eCFA immunization. **A,** The experimental design for (**B**) and (**C**), as described in Fig 1, *A*, was as follows: C57BL/6 WT mice were immunized with Ova plus distinct adjuvants and boosted with Ova without adjuvant on day 28 (n = 5 per group). **B,** The investigated adjuvants with their color codes. **C,** Data of the same experiment as shown in Fig 1. Serum titer of anti-Ova IgG, IgG subclasses, and IgM at the indicated time points (the serum dilutions used are shown). Vertical lines represent the Ova boost on day 28. **D** and **E,** Increased affinity of serum anti-Ova IgG Abs between day 8 and day 14 after Ova-eCFA immunization. **D,** The experimental design for (**E**) was as follows: WT mice were immunized with Ova-eCFA (n = 3 per group). **E,** Serum anti-Ova IgG binding ELISA (ELISA plates were coated with 10 or 1 μg/mL of Ova) of adjusted serum IgG titer from day 8 and 14 (similar extinctions when 10 μg/mL of Ova were coupled to the ELISA plate). Data are shown as mean values ± SEMs. *P < .05; **P < .01; ***P < .001; Student *t* test. One of 2 independent experiments is shown for each investigation.
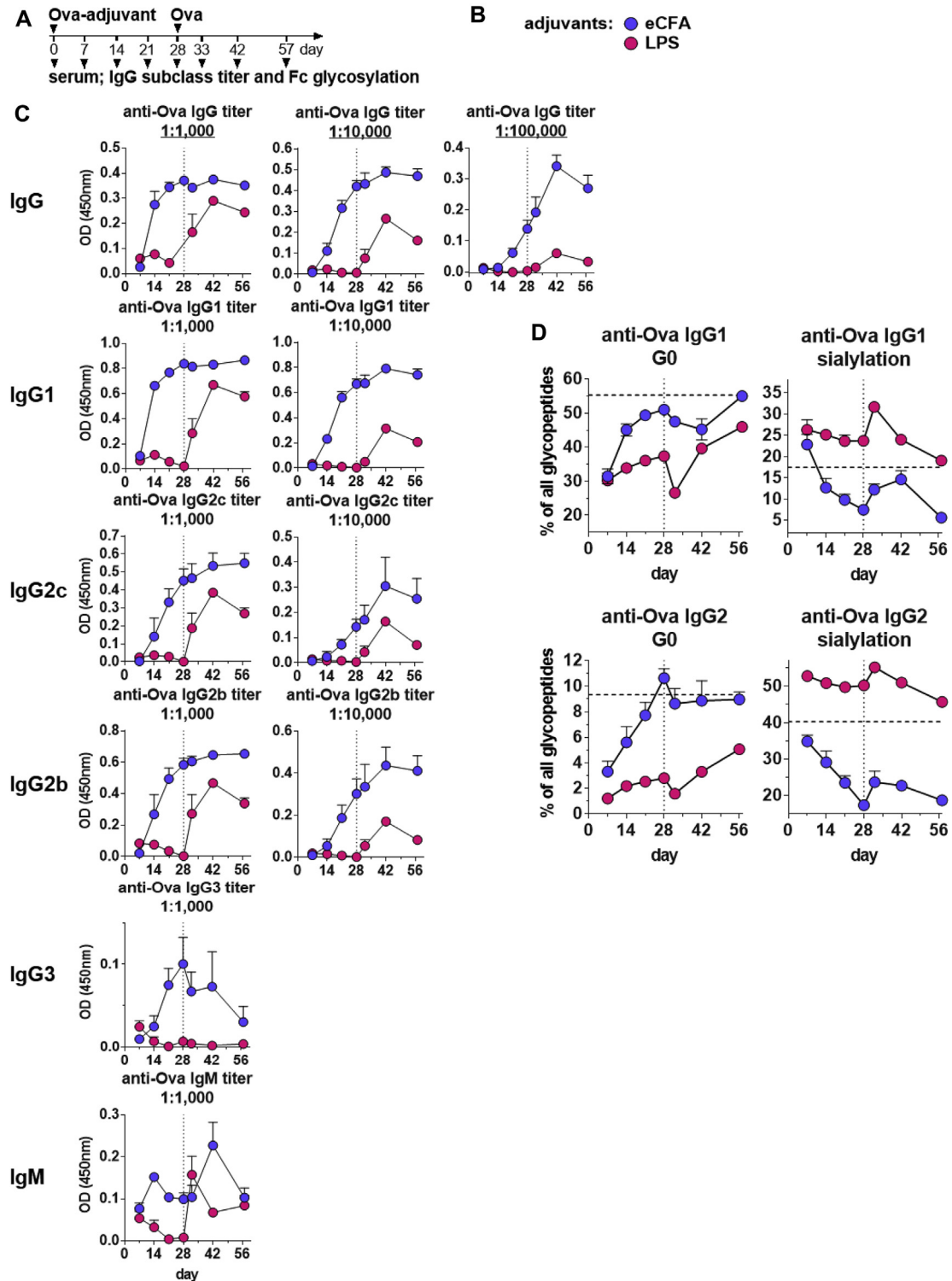
FIG E2. eCFA and LPS induce distinct IgG subclass titer and Fc glycosylation patterns after immunization with a foreign protein antigen. **A,** The experimental design for (**B**) to (**D**) was as follows: WT mice were immunized with Ova plus eCFA or LPS and boosted with Ova without adjuvant on day 28 (n = 5 per group). **B,** The investigated adjuvants eCFA and LPS with their color codes. **C,** Serum titer of anti-Ova IgG, IgG subclasses, and IgM on the indicated time points (the serum dilutions used are shown). Vertical lines represent the Ova boost on day 28. **D,** Serum anti-Ova IgG1 and IgG2 (IgG2c + IgG2b) Fc agalactosylation (percentages of the corresponding glycopeptide [G0]) and sialylation (G1S1 + G2S1 + G3S1 + G2S2) on the indicated time points. Horizontal dashed lines indicate average bulk serum IgG1 or IgG2 glycosylation before immunization. Data are shown as mean values ± SEMs. One of 2 independent experiments is shown.
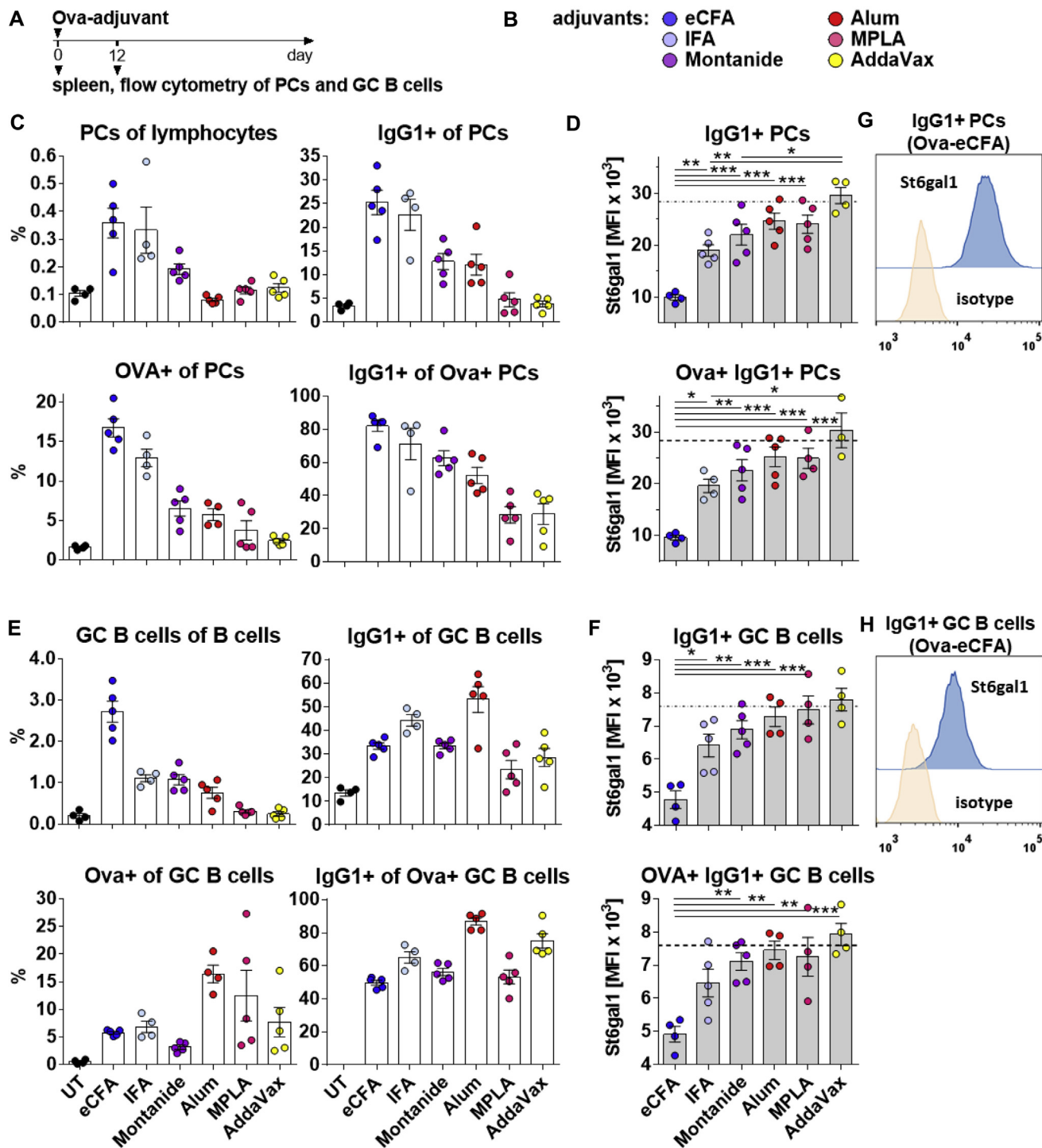
FIG E3. Adjuvants induce distinct St6gal1 protein expression levels in splenic IgG1^{+} PCs and GC B cells. **A,** The experimental design for (**B**) to (**F**) was as follows: WT mice were immunized with Ova plus different adjuvants and analyzed on day 12 (n = 5 per group). **B to F,** Data of the same experiment as shown in Fig 2. **B,** The investigated adjuvants eCFA, IFA, Montanide, alum, MPLA, and AddaVax with their color codes. **C,** Frequencies of splenic CD138^{+} PCs, IgG1-producing (IgG1^{+}) PCs among all PCs, Ova-specific (Ova^{+}) PCs among all PCs, and IgG1^{+} PCs among Ova^{+} PCs. **D,** Intracellular St6gal1 protein expression (median fluorescence intensity [MFI]) in splenic IgG1^{+} PCs and Ova[+] IgG1^{+} PCs. Horizontal lines indicate average St6gal1 expression levels in IgG1^{+} PCs of untreated mice. **E,** Frequencies of splenic GL7^{+} FAS^{+} GC B cells among B220^{+} CD138^{−} B cells, IgG1^{+} cells among all GC B cells, Ova-specific (Ova^{+}) cells among all GC B cells, and IgG1^{+} cells among Ova^{+} GC B cells. **F,** St6gal1 protein expression in splenic IgG1^{+} GC B cells and Ova[+] IgG1^{+} GC B cells. Horizontal lines indicate average St6gal1 expression levels in IgG1^{+} GC B cells of untreated mice. **G and H,** Representative overlay histograms of isotype compared with specific St6gal1 stainings of splenic (G) IgG1^{+} PCs and (H) IgG1^{+} GC B cells following immunization of WT mice with Ova-eCFA on day 12. Graph points indicate individual mice. Data are shown as mean values ± SEMs. *P < .05; **P < .01; ***P < .001; ANOVA. One of 2 independent experiments is shown. *UT,* Untreated.
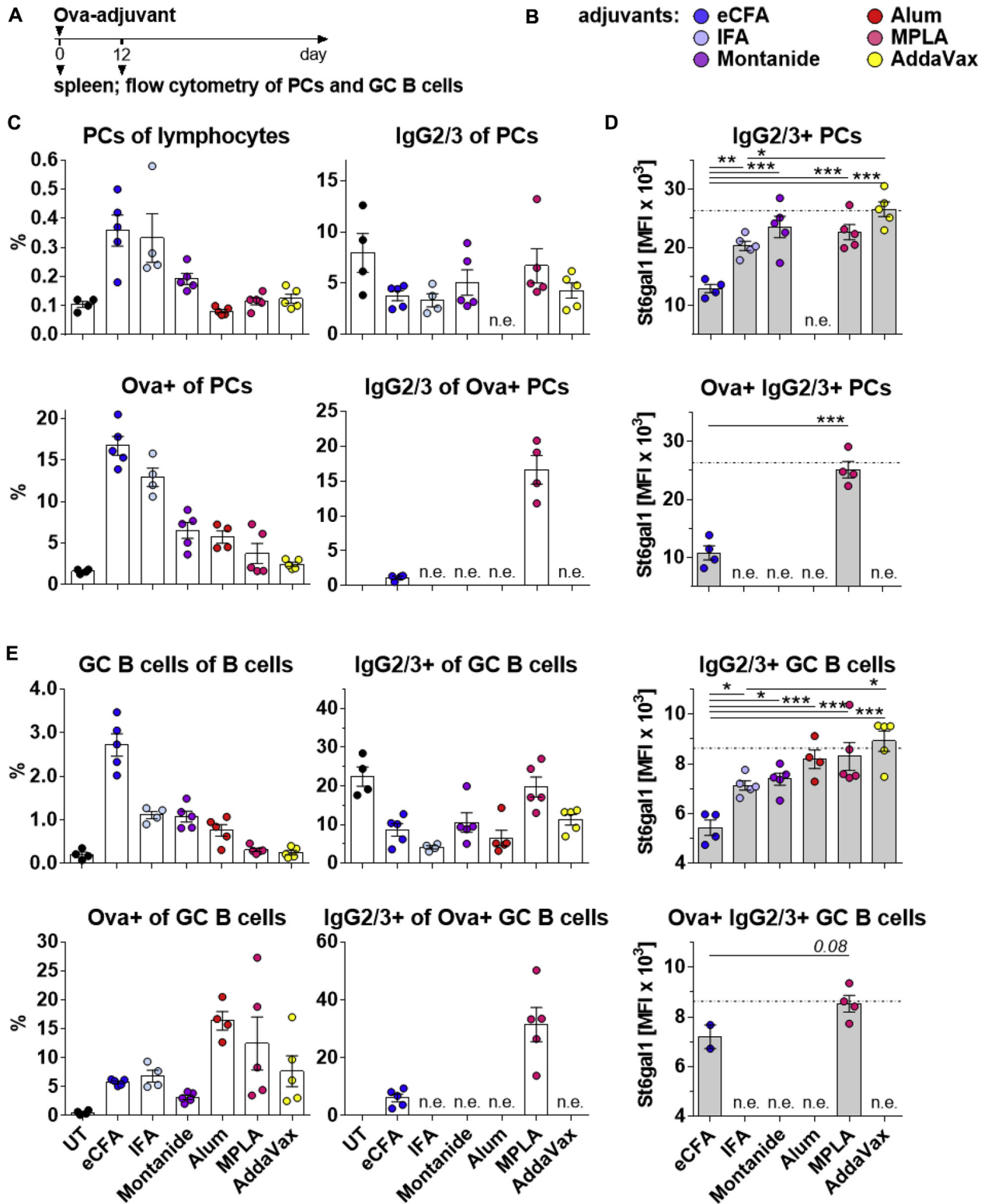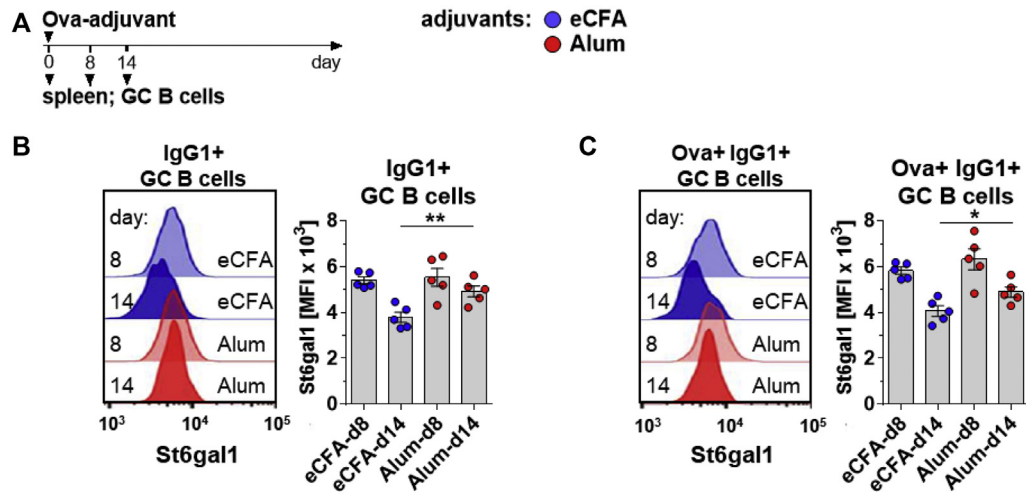
FIG E4. Adjuvants induce distinct St6gal1 protein expression levels in splenic IgG2/3⁺ PCs and GC B cells. **A,** The experimental design for (**B**) to (**F**) was as follows: WT mice were immunized with Ova plus different adjuvants and analyzed on day 12 (n = 5 per group). **B** to **F,** Data of the same experiment as shown in Fig 2 and Fig E3. **B,** The investigated adjuvants eCFA, IFA, Montanide, alum, MPLA, and AddaVax with their color codes. **C,** Frequencies of splenic CD138⁺ PCs, IgG/non-IgG1–producing (IgG2/3⁺) PCs among all PCs, Ova-specific (Ova⁺) PCs among all PCs, and IgG2/3⁺ PCs among Ova⁺ PCs. **D,** Intracellular St6gal1 protein expression in splenic IgG2/3⁺ PCs and Ova⁺ IgG2/3⁺ PCs. Horizontal lines represent St6gal1 expression of IgG2/3⁺ PCs from untreated mice. **E,** Frequencies of splenic GL7⁺ FAS⁺ GC B cells among B220⁺ CD138⁻ cells, IgG2/3⁺ cells among all GC B cells, Ova⁺ cells among all GC B cells, and IgG2/3⁺ cells among Ova⁺ GC B cells. **F,** St6gal1 protein expression in splenic IgG2/3⁺ GC B cells and Ova⁺ IgG2/3⁺ GC B cells. Graph points indicate individual mice. Data are shown as mean values ± SEMs. *P < .05; **P < .01; ***P < .001; ANOVA. One of 2 independent experiments is shown. *n.e.,* Not enough cells for reliable analysis; *UT,* untreated.
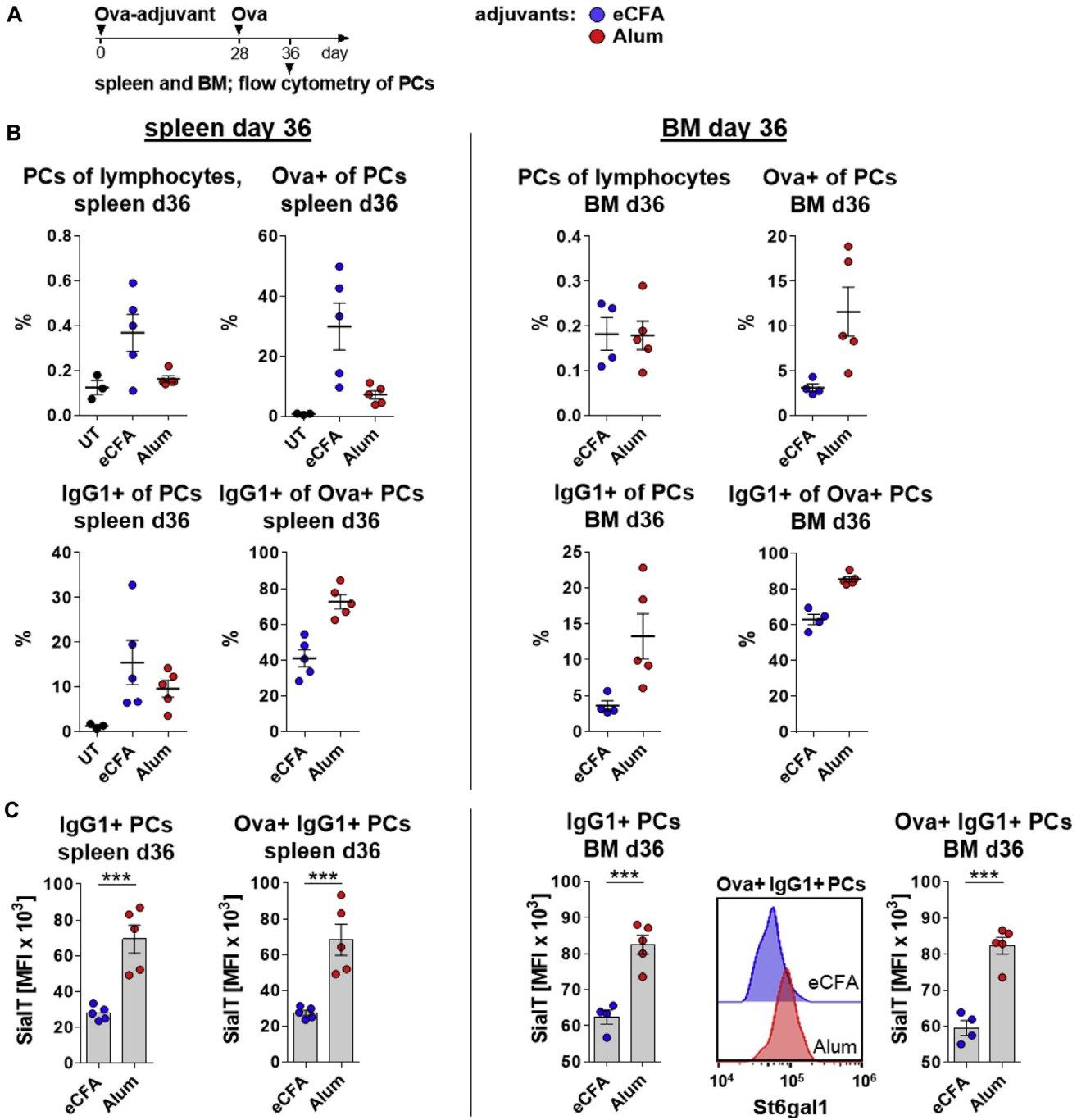
FIG E5. Ova-eCFA and Ova-alum induce distinct St6gal1 protein expression levels in splenic as well as BM IgG1^{+} PCs. **A,** The experimental design for (**B**) and (**C**) was as follows: WT mice were immunized with Ova plus eCFA or alum , boosted with Ova without adjuvant on day 28, and analyzed on day 36 (n = 5 per group). **B,** Frequencies of splenic (*left*) and BM (*right*) CD138^{+} PCs, anti-Ova Ab-producing (Ova^{+}) PCs among all PCs, IgG1-producing (IgG1^{+}) PCs among all PCs, and IgG1^{+}-producing PCs among Ova^{+} PCs on day 36. **C,** Intracellular St6gal1 protein expression in IgG1^{+} splenic and BM PCs and Ova[+] IgG1^{+} splenic and BM (including an overlay histogram of representative mice) PCs. Graph points indicate individual mice. Data are shown as means values ± SEMs. *P < .05; **P < .01; ***P < .001; Student *t* test. One of 2 independent experiments is shown.

FIG E6. Distinct St6gal1 protein expression levels in Ova-specific IgG1^{+} GC B cells subsequent to immunization with Ova-eCFA or Ova-alum on day 14, but not on day 8. **A,** The experimental design for (**B**) and (**C**) was as follows: WT mice were immunized with Ova plus eCFA or alum and analyzed on day 8 or 14 (n = 5 per adjuvant and time point). **B** and **C,** Intracellular St6gal1 protein expression in splenic IgG1^{+} (**B**) and Ova-specific (Ova[+]) IgG1^{+} (**C**) GC B cells (including overlay histograms of representative mice) subsequent to immunization on day 8 and 14. Graph points indicate individual mice. Data are shown as means ± SEMs. *$P < .05$; **$P < .01$; ***$P < .001$; 1-way ANOVA. One of 2 independent experiments is shown.
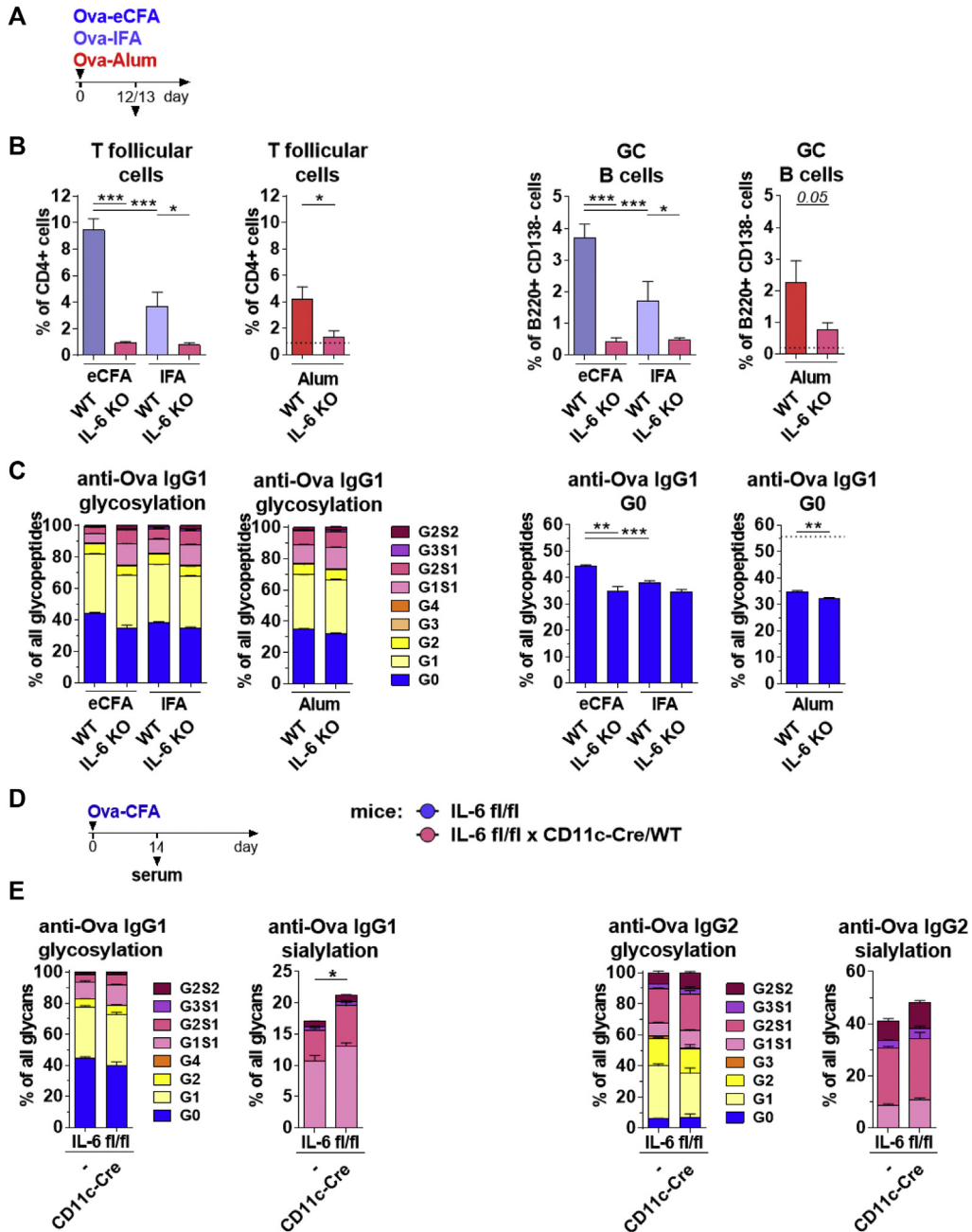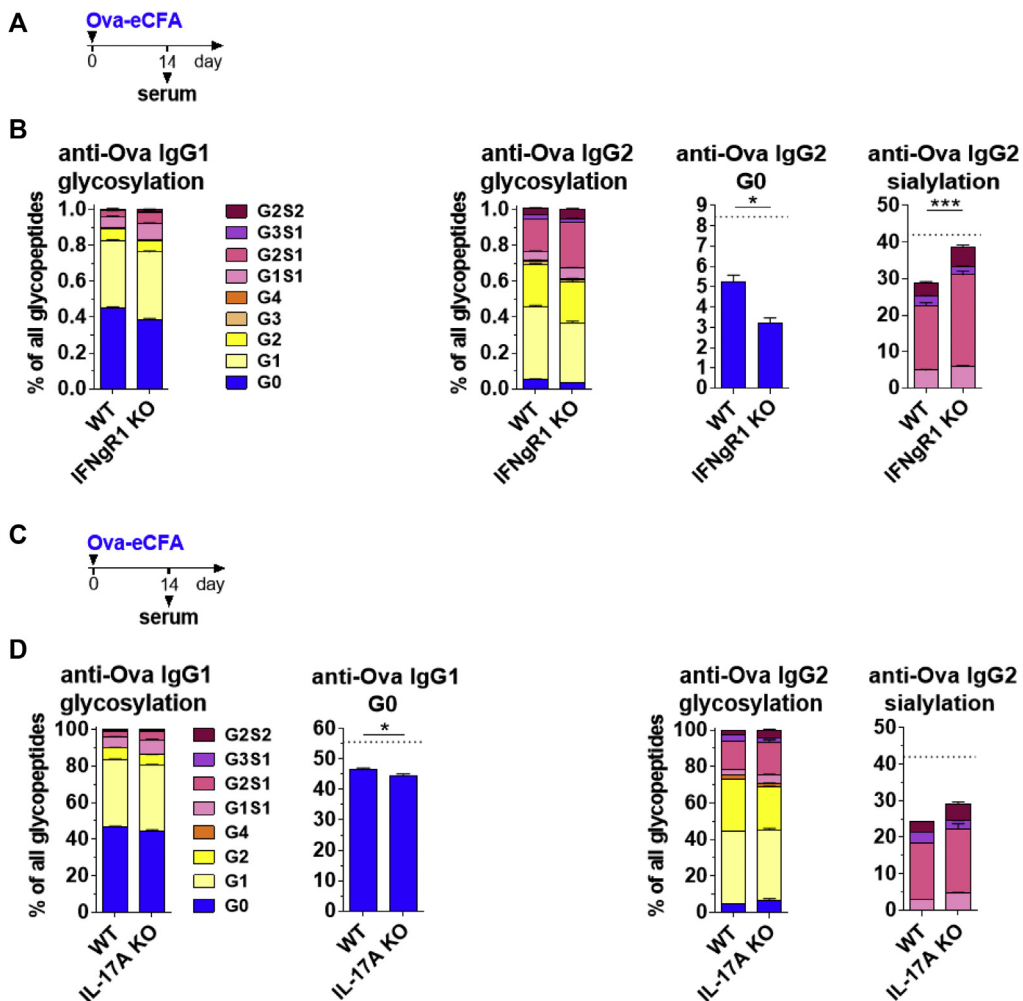
FIG E7. IL-6 downregulates IgG Fc galactosylation and sialylation subsequent to immunization with Ova-eCFA, Ova-IFA, and Ova-alum. **A,** The experimental design for (**B**) and (**C**) was as follows: WT and IL-6 KO mice were immunized with Ova-eCFA, Ova-IFA, or Ova-alum and analyzed on day 12 or 13 (n = 5 per group). **B** and **C,** Data of the same experiments as shown in Fig 3, K. **B,** Frequencies of splenic T follicular and GL7^{+} FAS[+] GC B cells. Horizontal dashed lines indicate average cell population frequencies of untreated mice. **C,** Serum anti-Ova IgG1 Fc total glycosylation (G0, G1, G2, G3, G4, G1S1, G2S1, G3S1, and G2S2) and agalactosylation (G0). The horizontal dashed line indicates average bulk IgG1 agalactosylation before immunization with Ova-alum. **D,** The experimental design for (**E**) was as follows: IL-6 fl/fl and IL-6 fl/fl × CD11c-Cre/WT mice were immunized with Ova-CFA and analyzed on day 14 (n = 6 or 7 per group). **E,** Serum anti-Ova IgG1 and IgG2 total glycosylation (G0, G1, G2, G3, G4, G1S1, G2S1, G3S1, and G2S2) and sialylation (G1S1, G2S1, G3S1, and G2S2). Data are shown as mean values with SEM. *P < .05; **P < .01; ***P < .001; 1-way ANOVA or Student t test. One of 2 independent experiments or 2 summarized independent experiments (C) (Ova-alum immunizations) are shown for each set of investigation.
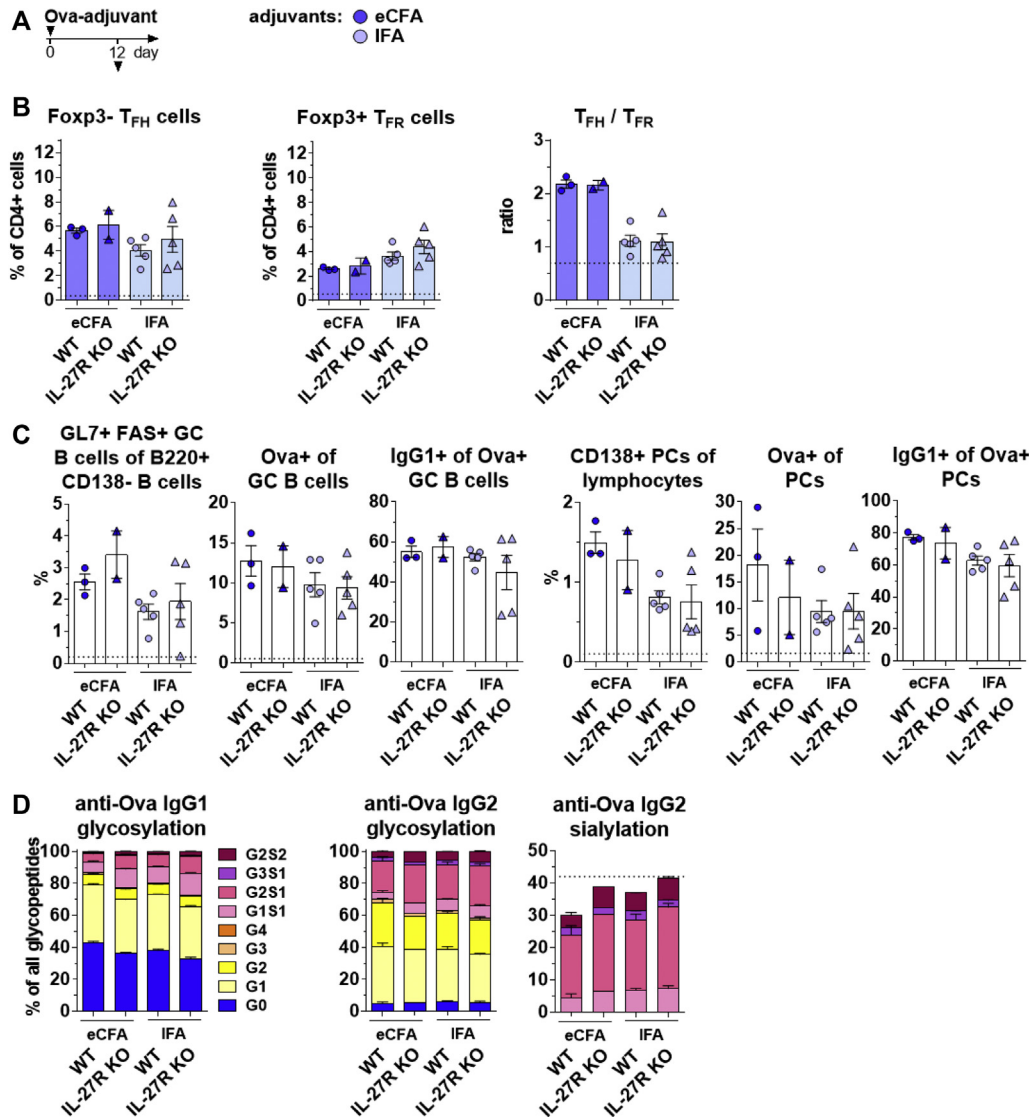
FIG E8. IL-27R signaling is necessary to induce IFN-γ–producing T_{FH1} cells and downregulate St6gal1 expression in GC B cells and PCs as well as serum anti-Ova IgG Fc galactosylation and sialylation. **A,** The experimental design for (**B**) to (**D**) was as follows: WT and IL-27R KO mice were immunized with Ova-eCFA or Ova-IFA and analyzed on day 12 (cell analysis, n = 2-5 per group; serum analysis, 3-5 per group). **B-D,** Data from the same experiment as shown in Fig 4, *B* to *F*. **B** and **C,** Frequencies of the indicated splenic CD4^{+} T-cell (**B**) and GC B-cell and PC (**C**) subpopulations. Horizontal dashed lines indicate average cell population frequencies of untreated mice. **D,** Serum anti-Ova IgG1 and IgG2 total glycosylation (G0, G1, G2, G3, G4, G1S1, G2S1, G3S1, and G2S2) and anti-Ova IgG2 sialylation (G1S1, G2S1, G3S1, and G2S2). The horizontal dashed line indicates average bulk IgG2 sialylation before immunization. There were not enough anti-Ova IgG2 data points for statistical analysis, but the trends for anti-Ova IgG2 sialylation between the different groups were comparable to the differences in anti-Ova IgG1 sialylation (Fig 4, *D*). Graph points indicate individual mice. Data are shown as mean values ± SEMs. One of 2 independent experiments is shown.

FIG E9. IFN-γ and IL-17A downregulate IgG Fc galactosylation and sialylation. **A**, The experimental design for (**B**) was as follows: WT and IFN-γRI KO mice were immunized with Ova-eCFA and analyzed on day 14 (n = 5 per group). **B**, Data from the same experiment as shown in Fig 4, *H*. Serum anti-Ova IgG1 and IgG2 (IgG2c + IgG2b) total glycosylation (G0, G1, G2, G3, G4, G1S1, G2S1, G3S1, and G2S2) and anti-Ova IgG2 agalactosylation (G0) and sialylation (G1S1, G2S1, G3S1, and G2S2). **C**, The experimental design for (**D**) was as follows: WT and IL-17A KO mice were immunized with Ova-eCFA and analyzed on day 14 (n = 4-7 per group). **D**, Data from the same experiment as shown in Fig 5, *H* and *I*. Serum anti-Ova IgG1 and IgG2 total glycosylation, anti-Ova IgG1 agalactosylation, and anti-Ova IgG2 sialylation. The horizontal dashed lines indicate average bulk IgG subclass agalactosylation or sialylation before immunization. Data are shown as mean values ± SEMs. *P < .05; **P < .01; ***P < .001; Student *t* test. One of 2 independent experiments is shown for each investigation.
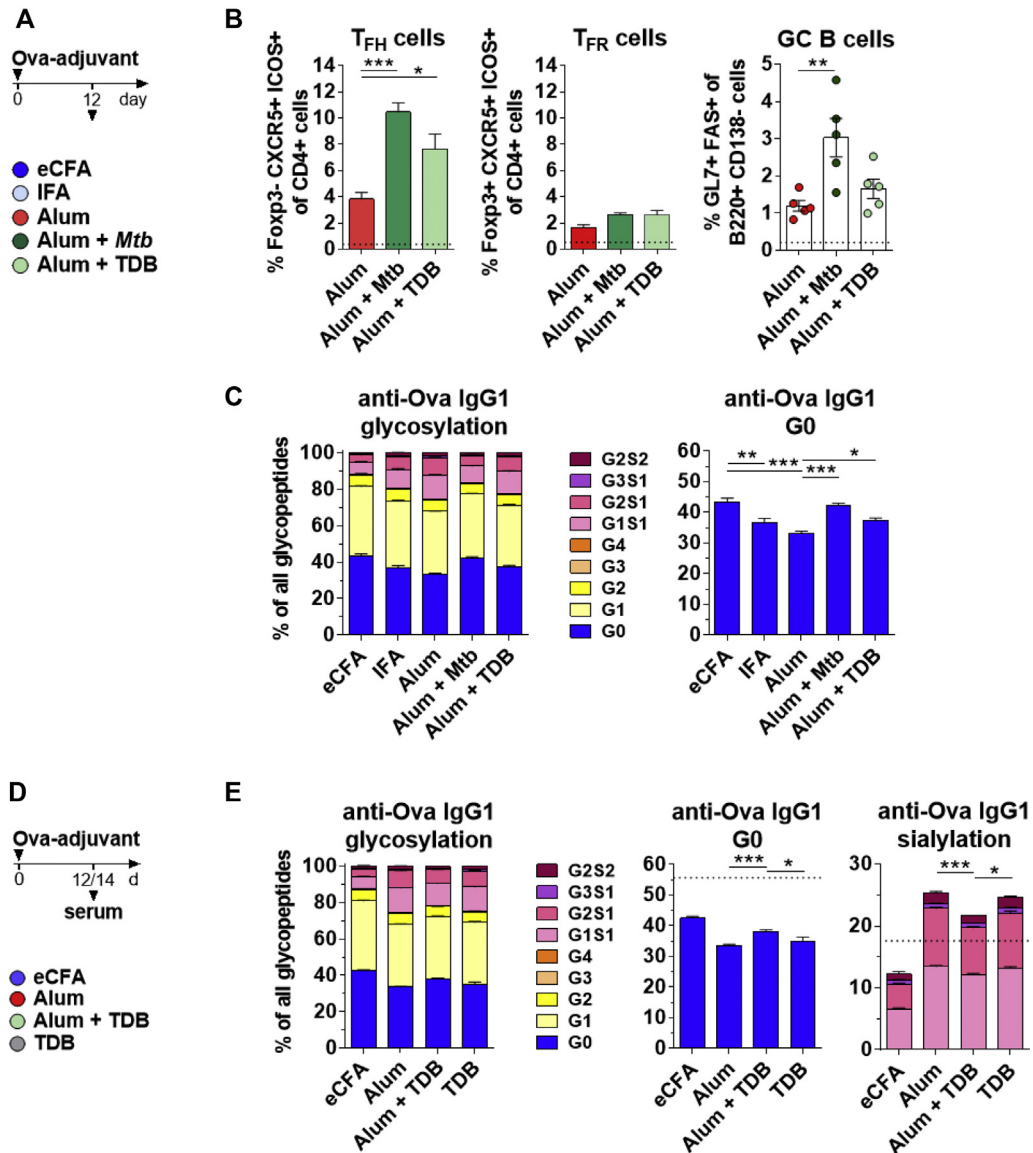
FIG E10. Mtb and TDB downregulate IgG Fc galactosylation and sialylation. **A,** The experimental design for (**B**) was as follows: WT mice were immunized with Ova plus eCFA, IFA, alum, alum + Mtb, or alum + TDB (TDB-HS15) and analyzed on day 12 (n = 5 per group). **B** and **C,** Data from the same experiment as shown in Fig 5, *J-M*. **B,** Frequencies of splenic Foxp3^{-} T_FH, Foxp3^{+} T_FR, and GC B cells. Horizontal dashed lines indicate average cell population frequencies of untreated mice. **C,** Serum anti-Ova IgG1 total glycosylation (G0, G1, G2, G3, G4, G1S1, G2S1, G3S1, and G2S2) and agalactosylation (G0). **D,** The experimental design for (**E**) was as follows: WT mice were immunized with Ova plus eCFA, alum, alum plus TDB, or TDB and analyzed on day 12 or 14 (n = 5 per group). **E,** Serum anti-Ova IgG1 total glycosylation (G0, G1, G2, G3, G4, G1S1, G2S1, G3S1, and G2S2), agalactosylation (G0), and sialylation (G1S1, G2S1, G3S1, and G2S2). The horizontal dashed lines indicate average bulk IgG1 agalactosylation and sialylation before immunization. Graph points indicate individual mice. Data are shown as mean values ± SEMs. *$P < .05$; **$P < .01$; ***$P < .001$; 1-way ANOVA. One of 2 independent experiments or 1 of up to 3 (**E**) summarized independent experiments is shown.
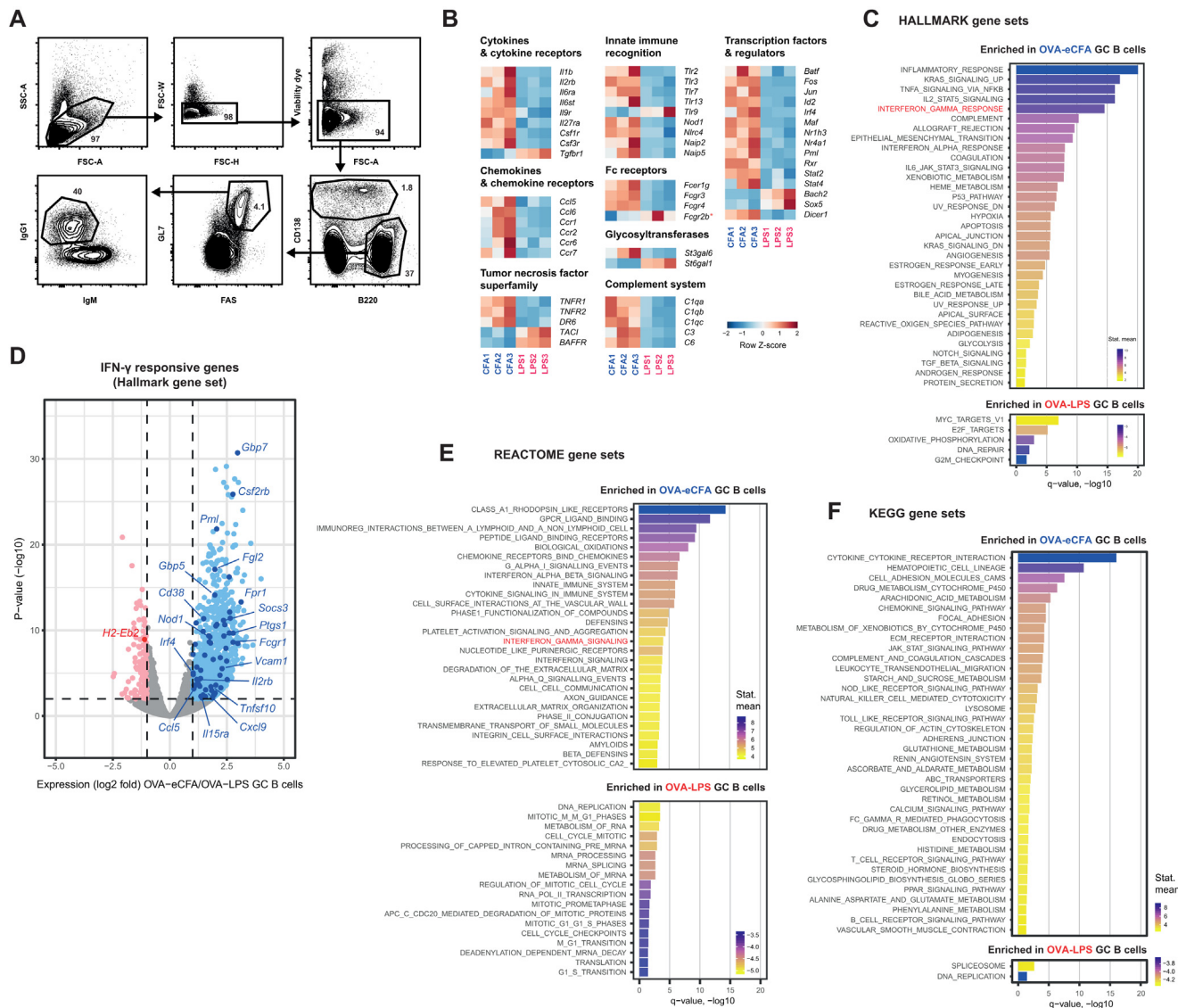
FIG E11. Adjuvants regulate the IgG1$^+$ GC B-cell transcriptome, including IFN-γ–responsive genes. Data from the same experiment as shown in Fig 6. **A,** Gating strategy for sorting splenic IgG1$^+$ IgM$^-$ GC B cells of Ova-eCFA– and Ova-LPS–immunized mice on day 8 (extracellular staining). **B,** A heatmap showing representative differentially expressed genes classified by function. **C,** A complete list of the hallmark gene sets significantly enriched ($q < 0.05$) in IgG1$^+$ GC B cells subsequent to Ova-eCFA or Ova-LPS immunization. The absolute value of the statistical mean represents the magnitude of gene set–level changes, and its sign indicates direction of the changes. **D,** P value–versus–log2 fold change "volcano" plot depicting IFN-γ–responsive genes (the hallmark gene set M5913) differentially expressed between Ova-eCFA– and Ova-LPS–induced splenic IgG1$^+$ GC B cells. **E and F,** Gene set enrichment results showing the gene sets from the Reactome (https://reactome.org/) (**E**) and KEGG (https://www.genome.jp/kegg/) (**F**) pathway databases that significantly enriched ($q < 0.05$) in IgG1$^+$ GC B cells following Ova-eCFA or Ova-LPS immunization.